

Review

# Remote Sensing Is Changing Our View of the Coast: Insights from 40 Years of Monitoring at Narrabeen-Collaroy, Australia

Kristen D. Splinter \*, Mitchell D. Harley and Ian L. Turner

Water Research Laboratory, School of Civil and Environmental Engineering, UNSW Sydney, Sydney 2052, Australia; m.harley@unsw.edu.au (M.D.H.); ian.turner@unsw.edu.au (I.L.T.)

\* Correspondence: k.splinter@unsw.edu.au

Received: 4 September 2018; Accepted: 31 October 2018; Published: 6 November 2018



**Abstract:** Narrabeen-Collaroy Beach, located on the Northern Beaches of Sydney along the Pacific coast of southeast Australia, is one of the longest continuously monitored beaches in the world. This paper provides an overview of the evolution and international scientific impact of this long-term beach monitoring program, from its humble beginnings over 40 years ago using the rod and tape measure Emery field survey method; to today, where the application of remote sensing data collection including drones, satellites and crowd-sourced smartphone images, are now core aspects of this continuing and much expanded monitoring effort. Commenced in 1976, surveying at this beach for the first 30 years focused on in-situ methods, whereby the growing database of monthly beach profile surveys informed the coastal science community about fundamental processes such as beach state evolution and the role of cross-shore and alongshore sediment transport in embayment morphodynamics. In the mid-2000s, continuous (hourly) video-based monitoring was the first application of routine remote sensing at the site, providing much greater spatial and temporal resolution over the traditional monthly surveys. This implementation of video as the first of a now rapidly expanding range of remote sensing tools and techniques also facilitated much wider access by the international research community to the continuing data collection program at Narrabeen-Collaroy. In the past decade the video-based data streams have formed the basis of deeper understanding into storm to multi-year response of the shoreline to changing wave conditions and also contributed to progress in the understanding of estuary entrance dynamics. More recently, ‘opportunistic’ remote sensing platforms such as surf cameras and smartphones have also been used for image-based shoreline data collection. Commencing in 2011, a significant new focus for the Narrabeen-Collaroy monitoring program shifted to include airborne lidar (and later Unmanned Aerial Vehicles (UAVs)), in an enhanced effort to quantify the morphological impacts of individual storm events, understand key drivers of erosion, and the placing of these observations within their broader regional context. A fixed continuous scanning lidar installed in 2014 again improved the spatial and temporal resolution of the remote-sensed data collection, providing new insight into swash dynamics and the often-overlooked processes of post-storm beach recovery. The use of satellite data that is now readily available to all coastal researchers via Google Earth Engine continues to expand the routine data collection program and provide key insight into multi-decadal shoreline variability. As new and expanding remote sensing technologies continue to emerge, a key lesson from the long-term monitoring at Narrabeen-Collaroy is the importance of a regular re-evaluation of what data is most needed to progress the science.

**Keywords:** Argus; lidar; coastal imaging; Unmanned Aerial Vehicle; RTK-GPS surveys; Google Earth Engine; CoastSnap; surfcams

## 1. Introduction

Narrabeen-Collaroy Beach, located on the Northern Beaches of Sydney along the Pacific coast of southeast Australia (Figure 1), is one of the longest continuously monitored beaches in the world ([1], see <http://narrabeen.wrl.unsw.edu.au/>). It complements a handful of other coastal monitoring programs around the world in which comprehensive datasets have been collected near-continuously using in-situ methods spanning several decades. Some notable examples of current long-term coastal monitoring programs worldwide include efforts by Rijkswaterstaat in the Netherlands (JarKus, <http://kml.deltares.nl/kml/rijkswaterstaat/jarkus/>), the United States Geological Survey on the US West Coast (e.g., [2]), the United States Army Corps of Engineers on the US East Coast (e.g., [3], see <http://www.frf.usace.army.mil/>) and the Hazaki Oceanographical Research Station in Japan (e.g., [4]). The international coastal research community has been using these long-term observations for more than four decades to significantly expand knowledge of nearshore processes, waves and beaches. Crucially, since the mid-2000s at Narrabeen-Collaroy, a rapidly expanding range of remote sensing tools and techniques have now taken over from in-situ methods as the primary data source for ongoing coastal monitoring.

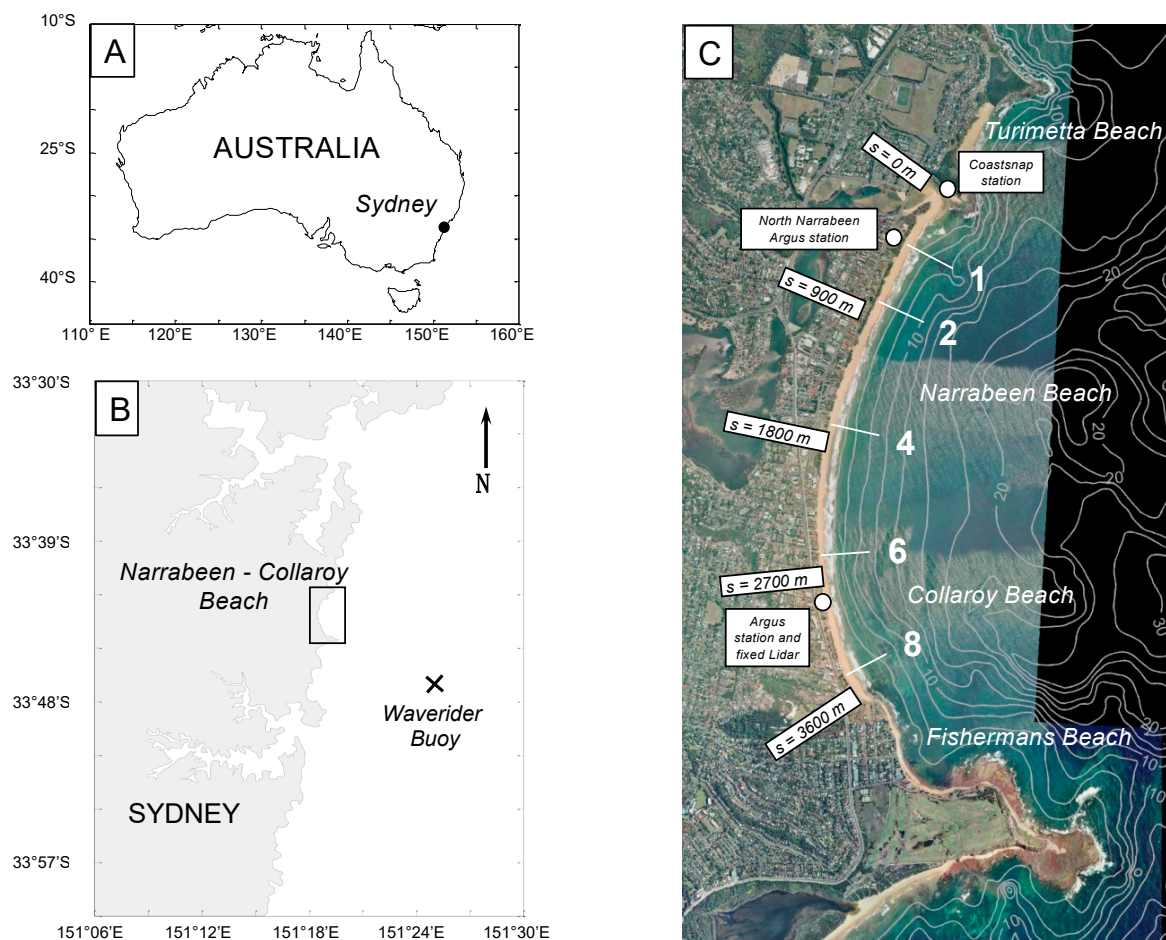


**Figure 1.** Location figure. (A) Location of Sydney in Australia. (B) Location of Narrabeen-Collaroy Beach within the Sydney region. (C) Narrabeen-Collaroy Beach, indicating the locations of the five historical survey profiles (1, 2, 4, 6 and 8) as well as the permanent and temporary Argus stations, fixed Lidar and CoastSnap station.

The purpose of this review paper is to present a broad overview of the evolving coastal monitoring technologies at Narrabeen-Collaroy and reflect on the role that remote sensing tools and techniques have played in driving the scientific impact of this globally-significant dataset. In this overview

we follow the chronology of the increasingly sophisticated data collection program. Significantly, since its inception in the mid-1970s, the more recent (2004) introduction of remote sensing techniques has greatly expanded the temporal and spatial resolution of these datasets that are now available for the site. This rapid expansion in data quantity, coverage and sophistication is summarized in Figure 2, where the exponential growth of the cumulative data collection program is summarized. To introduce the Reader to the Narrabeen-Collaroy site and monitoring program, in Section 2 we first discuss the pre-remote sensing era (1976–2004) during which conventional survey data was routinely collected. This earlier effort continues to underpin the value of the now greatly expanded ongoing monitoring program at Narrabeen-Collaroy. This is followed in Section 3 by more detailed descriptions of the progressive deployment of continuous automated remote sensing techniques, commenced in 2004, and how these technologies have advanced coastal science more broadly. As the wider coastal community continues to better understand coastal impacts to extreme events, in Section 4 we discuss the most recent shift in focus to event-based monitoring (2011–present), in which rapid mobilization of a range of remote sensing technologies are specifically deployed to capture unprecedented details of immediately pre- and post-storm beach response (Figure 2B). Throughout this paper we also highlight examples of notable scientific advances that the ever-growing datasets from Narrabeen-Collaroy and elsewhere have facilitated. Finally, in Section 5 Conclusions and Future Directions are provided.

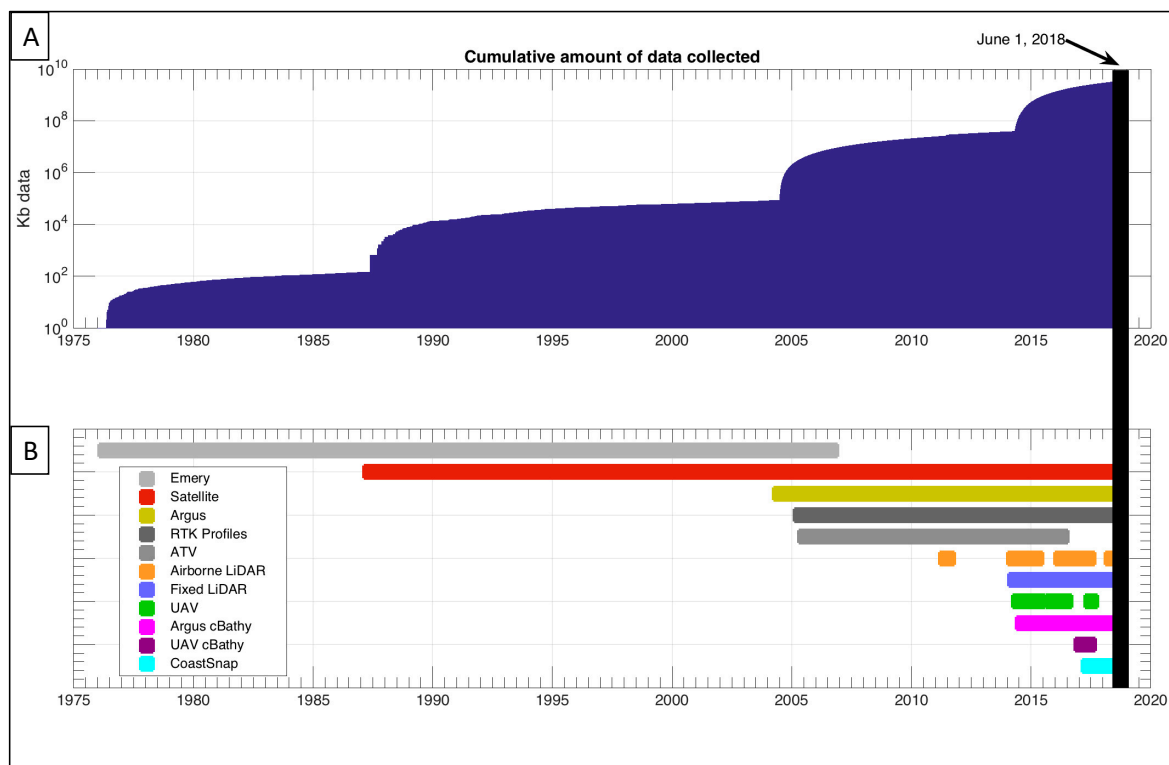


**Figure 2.** (A) Cumulative amount of data that has been collected at Narrabeen since 1976 as a function of different survey methods. (B) Timing of when platforms came online at Narrabeen. Greyscale—in-situ methods. Colors—remote sensing methods.

## 2. Pre-Remote Sensing Era at Narrabeen (1976–2004)

### 2.1. In-Situ Surveys (Emery Method)

At Narrabeen-Collaroy Beach, the initiation in 1976 of a continuing unbroken record of variability and change along an energetic, sandy coastline is due to the foresight and leadership of Professor Andrew (Andy) Short and his colleagues at the Coastal Studies Unit, University of Sydney. Since 2004, the continuing Narrabeen-Collaroy beach monitoring program has been maintained and significantly

expanded by researchers at the Water Research Laboratory, University of New South Wales (UNSW Sydney). For close to 30 years, the simple Emery method [5] was used to complete repeated cross-shore transect surveys (Figure 3A) within the 3.6 km long Narrabeen–Collaroy embayment (for further details of the site the Reader is referred to [1]). This early phase of the monitoring program was initially targeted at achieving fortnightly surveys at 14 transect locations that extended from the dune through the surfzone to the seaward side of the sandbar. Within a couple of years, the effort had refocused on monthly surveys at five representative transects locations (indicated in Figure 1C) extending from the toe of the dune to around the elevation of mean sea level. In hindsight, this early decision to limit the scope to an achievable and sustainable survey effort can now be seen as most likely the key reason this monitoring program was maintained, when so many others around the world have persisted for periods of up to several years, then ceased.

The profile data collected during this three-decade period of monthly surveys has contributed to a number of notable scientific contributions, including the formulation of what is now referred to internationally as the ‘Morphodynamic Beach State Model’ (discussed in Section 2.3), as well as early insights into rotation and oscillation at embayed beaches. Using these monthly profile data, Short et al. [6] and subsequently Short and Trembanis [7] detailed the approximately decadal-scale beach oscillation and rotation of the shoreline within the Narrabeen–Collaroy embayment (hereafter ‘Narrabeen’). Principal component analysis (PCA) revealed the two main components of variability at this beach. The dominant first component (PCA1), represents the temporal cross-shore oscillation of the mean shoreline position in response to individual storm erosion and recovery, whereas the second component (PCA2) reveals an underlying embayment-wide rotation that accounts for around 60% of the remaining shoreline variance. This early analysis suggested that the center of the embayment (i.e., Profile 4 in Figure 1C) represented a ‘pivot point’ or ‘fulcrum’ upon which beach sediment moved between. The northern and southern ends of the beach were shown to be negatively correlated to each other ( $r = -0.73$ ); as one end widens, the other narrows (Figure 3B), typically at timescales of 2 to 10 years. These rotations were hypothesized to be related to ENSO/SOI variability by Short et al. [6]; with the correlation of the observed embayment rotation to regional-scale climate forcing further explored in the work of Ranasinghe et al. [8] and Harley et al. [9]. These observations from Narrabeen–Collaroy of a likely link between regional-scale climate variability and coastline response parallels related work from other coastlines around the world. For example, Thomas et al. [10] reported decadal scale embayment rotation linked to the North Atlantic Oscillation (NAO) for a beach in Wales, while Barnard et al. [11] reported on a Pacific Basin study to examine the links between ENSO variability and enhanced coastal erosion at seasonal to annual scales. More recently, Anderson et al. [12] linked multi-decadal beach rotation along the Oregon (USA) coastline to both long-term climate indices (PDO) and shorter-term interannual signals (ENSO).

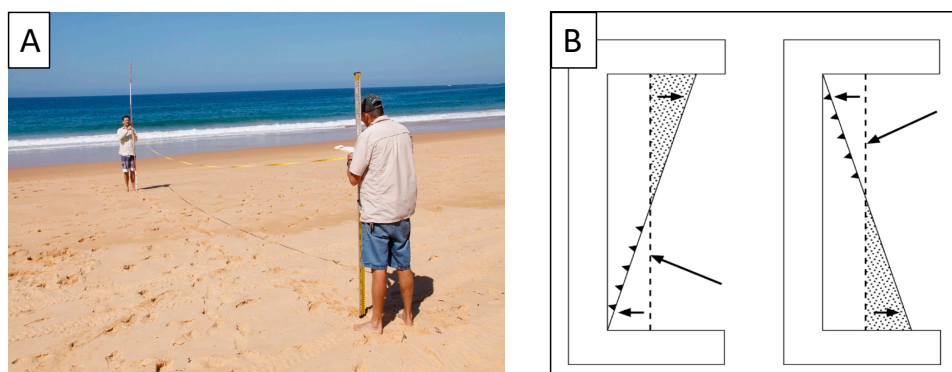


**Figure 3.** (A) Picture of Andy Short and Mitch Harley showing the Emery method (i.e., the use of a simple pole and tape measure) used to survey Narrabeen for the first 25 years (photo credit: Larry Paice). (B) A conceptual drawing of embayment beach rotation as described by Short and Trembanis (2004) (Source: [13]).

## 2.2. In-Situ Surveys (RTK-GPS and ATV)

With rapid improvements in the public availability of precision GPS technology and the increasing affordability of RTK-GPS survey equipment, data collection methods at Narrabeen advanced to more accurate and data dense delivery (Figure 4A). The historic five cross-shore profile lines continue to this day, with high-accuracy RTK-GPS replacing the original pole-and-tape Emery surveys since early 2005 [1]. Simultaneously, and continuing for a decade (2005–2016), these 2D profile surveys were complemented by the use of an all-terrain vehicle (ATV) to extend the routine coverage to include a full 3D (1 m cross-shore  $\times$  4 m alongshore) monthly survey of the entire subaerial embayment between the dune toe and mean sea level. To facilitate this transition from traditional surveys to the use of satellite positioning, Harley et al. [14] undertook a 16 month evaluation and comparison of the Emery and RTK-GPS methods at Narrabeen. Comparing 80 concurrent surveys, they found that the derived shoreline had a cross-shore standard deviation of error of 1.1 m, and the volume (above mean sea level) had a standard deviation of 3.6 m<sup>3</sup>/m. Overall, the 30 years of Emery method data was considered to be of very high quality, with a signal to noise ratio of 8.4, such that the error was significantly smaller than the observed variability.

Based on more than 30 years of the combined Emery (pre-2005) and continuing RTK-GPS profile dataset, Harley et al. [13] re-examined the initial PCA analyses [6,7] of embayment rotation at Narrabeen. The use of this extended dataset and new analysis methods clearly identified that the observed shoreline variance and rotation at Narrabeen is dominated (60% of the total shoreline variance) by the cross-shore (rather than alongshore) movement of sediment, occurring at different magnitudes from north to south due to a distinctive wave exposure gradient along the embayment (Figure 4A). Harley et al. [13] further determined that a secondary process of beach rotation (accounting for 26% of the total variance) is due primarily to the longshore transport of sediment, corresponding to regional-scale shifts in the offshore directional wave climate from south-east to east. In addition to the multi-year rotation signal that had been reported in earlier work, Harley et al. [13] also used this extended dataset to identify for the first time a distinct annual signal in the rotation component; highlighting the importance of sustained and long-term monitoring programs at sufficient temporal resolution to provide insight that shorter duration measurements simply cannot reveal.

In the most recent extension of the ongoing beach rotation research at Narrabeen, Harley et al. [15] used five years of the ATV-derived full 3D embayment RTK-GPS dataset to re-examine the role of cross-shore sediment transport processes. The ATV data set has a survey spatial resolution of order 5 m in the direction of ATV travel, with alongshore 'transects' spaced roughly every 2–5 m in the cross-shore. The raw survey data is then interpolated to a regularly-spaced finer mesh grid. Their analyses confirm that the dominant forcing of shoreline variability within the 3.6 km Narrabeen embayment is the result of cross-shore processes, which vary alongshore due to distinct alongshore gradients in inshore wave energy caused by the sheltering effect of the adjacent and prominent headlands. A steepening and flattening of the inter-tidal beach slope (measured from the berm to mean sea level) was also revealed, which is hypothesized to result from the dissipation of wave energy caused by observed variations in the cross-shore location of sandbars. An enhanced conceptual model of beach rotation was proposed, in which the explicit role of sandbars as well as wave direction and energy are included for the first time.

Bracs et al. [16] extended this thinking to two beaches along the NSW coastline to compare regional synchronous behavior between embayed beaches with similar orientations. Using three years of monthly RTK-GPS 3D embayment surveys, they found that Narrabeen and Wamberal beaches, separated by 35 km, had very similar timescales and spatial patterns of beach shoreline change over this three-year period. Both beaches were dominated by oscillation, rather than rotation, in agreement with previous work by Harley et al. [15]. Similar coherent spatial and temporal patterns of the two beaches were also observed at the individual storm timescale.

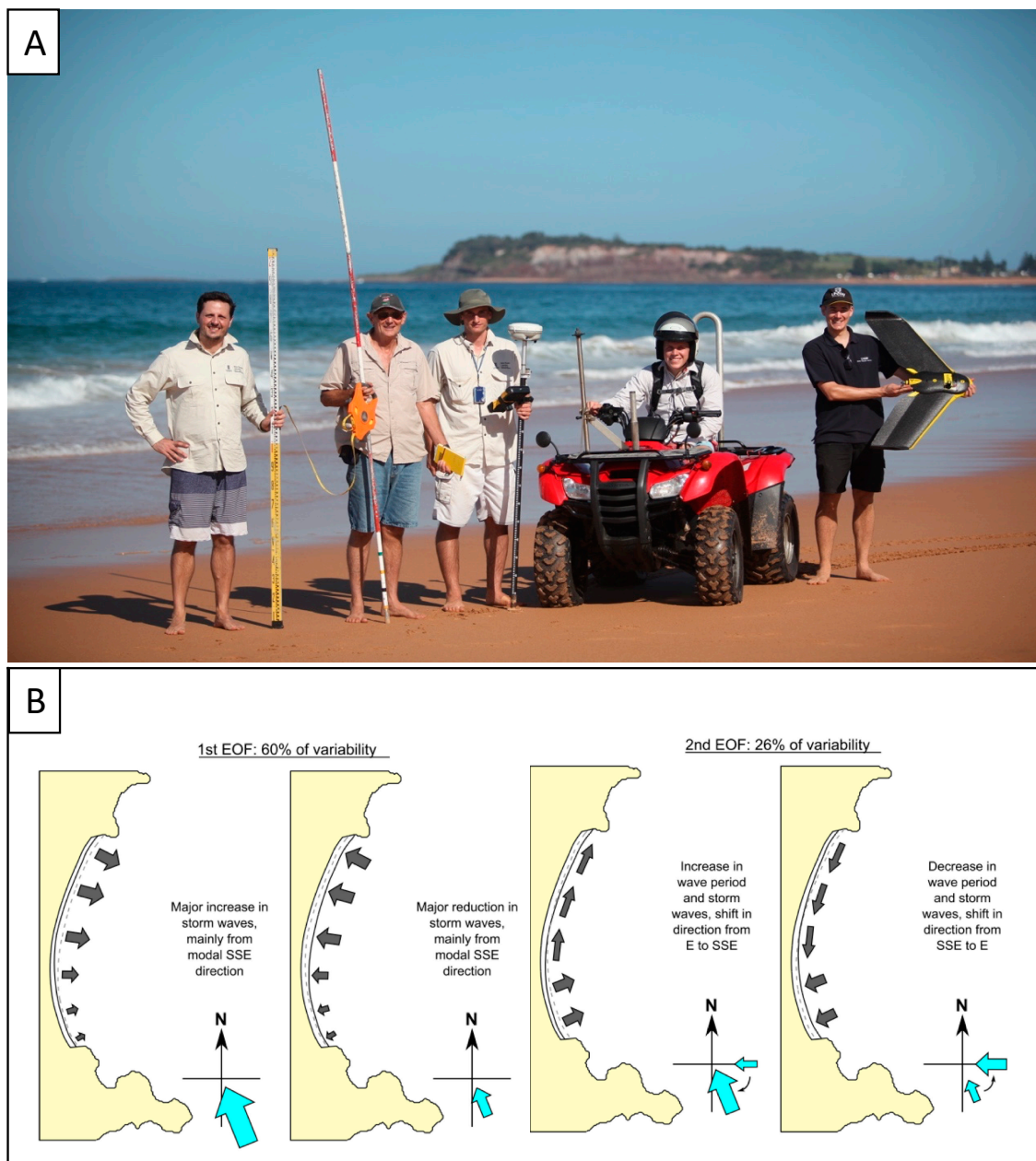


**Figure 4.** (A) Picture of survey methods with (l-r) Emery Method, RTK-GPS, all-terrain vehicle (ATV) RTK-GPS and Unmanned Aerial Vehicle (UAV) (photo credit: Larry Paice). (B) New insights into embayed beach rotations (Source: [13]).

### 2.3. The First 'Remote Sensors' at Narrabeen-Collaroy: Visual Classification of the Surf Zone

The first reported instances where 'remote sensing' was employed at Narrabeen-Collaroy are encapsulated in the landmark papers of Wright and Short [17] and Wright et al. [18], in which detailed visual observations from around the Narrabeen-Collaroy embayment were key to the formulation by these authors of new ideas demonstrating the interdependence of hydrodynamics and morphology (i.e., 'morphodynamics') at beaches. Much of the visual patterns of wave breaking that assisted in the genesis of these ideas were documented from vantage points along the beach and adjacent headlands at Narrabeen, complimented by observations from other coastal sites around Australia. The resulting six commonly identified 'Morphodynamic Beach States' observed at micro-tidal beaches (Figure 5) identified and described by Wright and Short [17]. At Narrabeen-Collaroy, the more sheltered southern

end of the embayment (refer Figure 1C) predominately displays the lower to moderate energy beach states (refer Figure 5) of Reflective, Low Tide Terrace, Transverse Bar and Rip and Rhythmic Bar and Beach. During storms and at the more exposed northern end of the beach, beach states can transition to Longshore Bar and Trough and, on rare occasions, high-energy Dissipative conditions. During periods of more quiescent wave energy, a downshift in beach states along the embayment is observed [18].

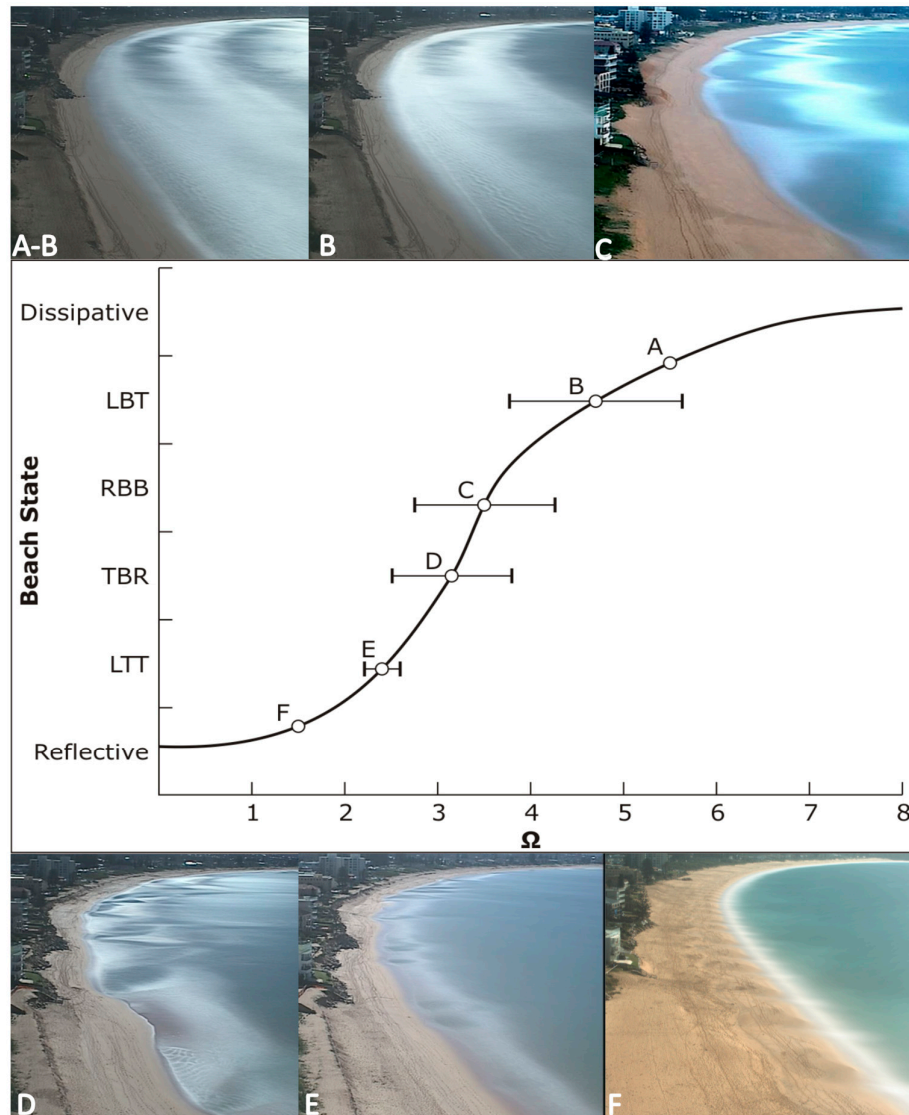


**Figure 5.** The full range of Morphodynamic Beach States observed at Narrabeen-Collaroy using the Argus station. (top, l-r) Example images of instantaneous beach states. (A,B): Dissipative—Longshore Bar Trough (LBT); (B): Longshore Bar Trough; (C) Rhythmic Bar Beach (RBB). (middle) Beach state as a function of dimensionless fall velocity ( $\Omega$ ). (bottom, l-r) (D) Transverse Bar Rip (TBR); (E) Low Tide Terrace (LTT); (F) Reflective.

This beach state model was later expanded by Lippmann and Holman [19,20], who used video imagery from Duck, North Carolina (USA). They identified 8 morphological classifications, separating morphology into incident and infragravity length scales as well as alongshore rhythmic and non-rhythmic features. This focus within the international literature on the classification of characteristic beach states located along wave-dominated micro-tidal coasts was subsequently expanded by Masselink and Short [21], who introduction of the concept of a relative tide range to extend these same concepts to include macro-tidal coastlines.

#### 2.4. Developments in Video-Based Remote Sensing in the USA and Europe

Prior to the installation of continuous video-based monitoring at Narrabeen in 2004, two decades earlier groups in both the USA and Europe began to experiment with video-based remote sensing methods to monitor the nearshore region [19,22]. Here we focus on the Argus camera system developed by Professor Robert (Rob) Holman of the Coastal Imaging Laboratory at Oregon State University, as this is the system that was subsequently adopted in Australia and much of the scientific literature. The Argus camera systems, originally recording to VHS tapes, have since evolved with technology into the digital era [23,24]. Fundamental to the use of oblique image pixels to the quantitative analyses of the nearshore was the development of routine tools that enable the researcher to rectify and georeference images to real-world coordinate systems to within (sub)meter accuracy, accounting for factors including lens distortion, camera roll, image centers and scale factors [25]. A summary of the key processes that have been examined by video remote sensing and examples of related publications are provided in Table 1 and further described within the context of the scientific advancements at Narrabeen described in Section 3.

### 3. Automated Remote Sensing to Expand Routine Monitoring at Narrabeen-Collaroy (2004–Present)

#### 3.1. Video-Based Remote Sensing at Narrabeen

Video-based remote sensing using Argus arrived in Australia in the early 2000s and was first installed at Narrabeen-Collaroy in 2004 [26] and is still in operation today. Using a 5-camera system, a permanent Argus station located towards the southern end of the embayment at Collaroy (refer Figure 1C) captures the southern half of the full 3.6 km long beach (Figure 6A). A second temporary Argus station was also installed at North Narrabeen (refer Figure 1C) to monitor the lagoon entrance and adjacent beach at the northern end of the embayment (Figure 6B), that remained in operation between 2005 and 2008. In line with all Argus systems currently operating worldwide, a range of video-derived data products have been routinely collected, including 10-min time-exposure (timex) images; instantaneous snapshots (snaps); variance images (var); min and max intensity; runup lines; and more recently full video used to derive celerity-based bathymetry by applying the cBathy technique [27].



**Figure 6.** (A) The permanent Narrabeen Argus cameras system atop the Flight Deck Building that has been in operation since 2004. (B) The temporary North Narrabeen Argus cameras installation atop the North Narrabeen Surf Life Saving Club, that operated between 2005–2008.

**Table 1.** Key international research outcomes provided by video remote sensing.

Process	Example Publications
Shoreline behavior	Alexander and Holman [28]; Turner et al. [29]; Davidson and Turner [30]; Davidson et al. [31]; Splinter et al. [32–34]; Pianca et al. [3]
Sandbar behavior	Plant et al. [35]; Van Enckevort and Ruessink [36,37]; Ruessink et al. [38]; Castelle et al. [39]; Pape et al. [40]; Splinter et al. [41]; Splinter et al. [42]
Nearshore morphology	Lippmann and Holman [19,20]; Price and Ruessink [43,44]
Nearshore bathymetry	Stockdon and Holman [45] Aarninkhof [46]; Holman et al. [27]
Inter-tidal topography	Holland and Holman [47]; Plant and Holman [48]; Aarninkhof et al. [49,50]; Uunk et al. [51]; Didier et al. [52]
Tidal inlet dynamics	Pianca et al. [53]; Harrison et al. [54]
Rip current location and persistence	Holman et al. [55]; Turner et al. [56]; Quartel [57]
Nearshore wave celerity	Holland and Holman [58]; Stockdon and Holman [45]; Plant et al. [59]
Nearshore wave angle	Holman and Chickadel [60]
Nearshore wave dissipation	Aarninkhof and Ruessink [61]
Nearshore longshore currents	Chickadel et al. [62]
Wave height from stereo pairs	de Vries et al. [63]; Shand et al. [64]
Swash characteristics	Stockdon et al. [65]; Power et al. [66]; Senechel et al. [67]; Palmsten and Splinter [68]
Dune erosion	Palmsten and Holman [69]

To facilitate the direct integration of these newly available image-derived monitoring products with the existing RTK-GPS survey program at Narrabeen, Harley et al. [14] used 307 images to derive remotely sensed shorelines and undertaken a comparison of accuracy relative to the monthly RTK-GPS in-situ surveys conducted between July 2005 and December 2006. The remotely sensed shorelines included elevation correction for tide and waves. The resulting shorelines were shown to have a cross-shore standard deviation of error of 1.2 m when compared to RTK-GPS surveys, with errors increasing further away from the cameras due to decreasing image resolution. Overall, it was concluded that the cameras provide measurements of high-accuracy daily shoreline variability along the beach that are comparable to in-situ methods.

The continuous (daylight hours) images collected by the permanent Argus station provide very high temporal and spatial resolution data to explore key morphodynamic processes that were not previously captured by the monthly profile or ATV surveys undertaken at this site. In addition, the use of automated camera systems also facilitates ‘retrospective’ observations and analyses of rapid coastal change, providing assurance that no significant events at a site are ‘missed’. And very importantly, the adoption of the ‘standard’ Argus platform at Narrabeen has facilitated collaboration and the broader use of the growing image database within the international coastal imaging research community.

The approximately one and a half decades of video-derived data timeseries that are now available at Narrabeen have been used for a broad range of applications, including: improved understanding in inter-tidal morphology dynamics [70]; individual storm response of shorelines [71,72]; exploration into the key drivers of annual to decadal shoreline response [31,32]; calibration data sampling requirements for shoreline modelling [73]; the role of sandbars in beach recovery [74] and beach state dynamics [75]. These studies and the contributing role of the available remote-sensed data are further described below.

### 3.1.1. Coastal Lagoon Entrance Sediment Dynamics

Undertaking repeated and frequent in-situ surveying of inter-tidal areas in estuaries and tidal lagoons is challenging and alternative methods of continuous monitoring are required. The North Narrabeen Argus station (2005–2008) complemented approximately one year of intense (weekly to bi-weekly) kayak and wading RTK-GPS surveys of the lagoon entrance to monitor infilling after a mechanical entrance clearing operation in December 2006. Using the hourly time-exposure (timex) images collected by this temporary Argus station that were first validated by the less frequent in-situ surveys, Morris et al. [70] reported on a high accuracy method (vertical error of 0.05 m) to automatically map inter-tidal bathymetry in estuaries using the waterline technique.

Following a mechanical opening of the Narrabeen lagoon entrance in July 2006, Morris et al. [70] show that the infilling of sand into the coastal lagoon system over the following month occurred predominately from the ocean side, as a result of wave action and longshore currents closing the lagoon entrance. Interestingly, video derived shorelines showed that there was no significant change in the morphology of the flood shoal during this opening and closing event due to the available 'accommodation space' for sand to be deposited and ebb flows unable to provide the necessary scour. Storm wave events, catchment discharge and the location of the divergence point of the flood tidal delta were all found to be key factors in the morphodynamic evolution of this ICOLL ('intermittently closed and open lake/lagoon') entrance.

The successful application of video-based monitoring of the lagoon entrance at Narrabeen supports similar studies from other sites around the world, highlighting the advantages of this technology to the understanding of morphological processes at tidal inlets and mud flats. For example, Pianca et al. [53] used 23 days of video-derived time-exposure (timex) images to monitor the migration and evolution of meso-scale morphology on a micro-tidal ebb delta in New River Inlet, North Carolina. Using a Lagged Least Square Algorithm, they were able to track the movements of these features (denoted by wave breaking patterns) and found a very complex circular migration pattern as these features moved offshore and away from the inlet in offshore regions and then back towards the inlet in the nearshore, consistent with residual flow patterns of an ebb-tidal delta. Mean migration rates derived from these video-based measurements were of the order 1–2 m/day. Similarly, Harrison et al. [54] reported on a 5-year study of an ebb-tidal delta at Raglan, New Zealand using video observations of depth-limited wave breaking patterns. They too found that movement of the ebb-tidal features were linked to hydrodynamic (waves and tides) conditions. Their longer study also found that the system was more dynamic during seasonal shifts in forcing.

### 3.1.2. Shoreline Response to Storms

Video remote sensing has advantages over traditional in-situ surveys as it automatically captures high spatial and temporal resolution data that can be used to further observe and understand rapid adjustment of beaches to storms. Harley et al. [71] utilized approximately 5 years of timex and variance image data collected from both the North Narrabeen and Narrabeen Argus stations to determine immediately pre- and post-storm shorelines at the more exposed (northern) and sheltered (southern) regions of the 3.6 km long embayment. These observations were used to develop an empirical relationship for shoreline storm demand at Narrabeen-Collaroy, where change in beach width ( $\Delta W$ ) is a function of the cumulative wave energy of the storm ( $E$ ). Unique to image data whereby both the cross-shore position of the shoreline and sandbar(s) can be readily obtained, these authors identified three distinct classes of erosion potential as a function of cumulative storm energy. Exposed beaches absent of offshore sandbar morphology were most susceptible to erosion, followed by partially-exposed and barless beaches, with sheltered and/or barred profiles the least vulnerable. It was also observed that the southern, more sheltered end of the beach was more sensitive to storm wave direction than the northern end, highlighting the morphological complexity of embayed beaches. Kearney et al. [76] subsequently applied this same methodology to 83 storm events at the Gold Coast, (Queensland, Australia) where video-derived shorelines and sandbar locations were also available. While they

found similar trends in increasing cumulative storm energy resulted in greater shoreline erosion, beach morphology state was also found to play an important role at this longshore drift coastline. Higher energy beach morphodynamic states [17] resulted in less erosion for the same amount of storm energy when compared to Narrabeen's embayed coastline. Both studies followed the reasoning first mooted by Wright and Short [17,18] whereby more dissipative beaches (i.e., wide and barred profiles) are more in equilibrium with higher energy wave conditions, and are therefore most resilient to short-term erosive storm events.

Recently, Beuzen et al. [72] extended on Harley et al.'s (2009) earlier empirical analysis by using 10-years of shoreline data (totalling 137 individual storms) obtained from the permanent Argus station at Narrabeen-Collaroy, to develop a Bayesian Network (BN) to predict shoreline erosion response to storms. Their network incorporated more variables than Harley et al. [71], including information about the prevailing beach state, water levels and storm independence, but also allowed for a probabilistic outcome, rather than a deterministic (single answer) value. Using a variance reduction technique, they identified that the 2 most important variables in explaining the shoreline response to forcing were: (1) cumulative nearshore wave power; and (2) pre-storm beach width. These results are consistent with earlier work from both Australia and the USA (e.g., [31,71,77,78]) where shoreline change is related to both immediate forcing and antecedent beach state. A maximum predictive skill of the model on unseen data was found to be 65% for a 2-node network. Higher predictive skill could be achieved (up to 88%) on the training data set when the model was allowed to be overfit. Using this unique dataset, Beuzen et al. [72] also usefully describe the differences between descriptive and predictive BN models, providing guidance to future modelers on the type and amount of data needed to reliably use BNs for a broader range of coastal applications.

### 3.1.3. Shoreline Modeling

Video remote sensing data provides a unique source of long-term, sustained monitoring of the coastline, in which shoreline behavior can be explored in relation to a range of forcing conditions [3,31,33]. Utilizing approximately six years of weekly image-derived shoreline data from the permanent Argus station at Narrabeen-Collaroy, Davidson et al. [31] developed and tested a new equilibrium-based shoreline model for wave-dominated coastlines. Based on this continuous and multi-year dataset, the model was shown to capture the individual storm response as well as the observed seasonal to inter-annual variability with a reasonable degree of skill ( $0.57 < r^2 < 0.66$ ). A novel contribution of this work was the inclusion of the concept of a time-varying dynamic equilibrium in shoreline position based on the earlier concepts of Wright et al. [18]. These new results showed that storm-dominated beaches (such as Narrabeen) tend to have a short 'memory' such that the prevailing equilibrium shoreline position is primarily a function of short-term (i.e., days to weeks) past wave conditions. In contrast, more energetic and seasonally-dominated beaches were shown to have a much stronger dependence on longer-term (more than 1 year) equilibrium conditions, with these beaches tending to predominately oscillate around a time-invariant mean shoreline position.

Acknowledging the unique aspect of having a daily timeseries of multi-year, remote sensed (video) data available to test and train their models at Narrabeen-Collaroy, Splinter et al. [73] explored the key question of how much data (sampling frequency and duration) is necessary to train equilibrium-based shoreline models. Using data obtained from the permanent Narrabeen-Collaroy Argus station at this storm-dominated site, as well as a second station also located on Australia's eastern coastline at the seasonally-dominated Gold Coast in Queensland, it was found that sampling requirements for model calibration are a function of the primary mode of beach variability. At storm-dominated beaches such as Narrabeen-Collaroy, where storms occur on average every two to four weeks, fortnightly shoreline measurements for a minimum period of two years are found to be necessary to achieve an acceptable degree of predictive model skill. In contrast, at more seasonally-dominated sites, monthly sampling for a minimum of 2 years is required to adequately capture the range of dynamic variability of the observed shoreline. At many sites world-wide this intensity of in-situ surveying would be challenging

to maintain due to logistics and cost, emphasizing the practical use of remote sensing methods as an attractive alternative to inform model development and calibration.

Splinter et al. [32] utilized remotely-sensed video data from Narrabeen as well as comparable timeseries of (mostly video-derived) shoreline data from six additional sites around the world to examine generic relationships between model free parameters in an equilibrium shoreline model and the dominant morphology and wave forcing at each site. Individual site characteristics ranged from micro-tidal, moderate energy beaches such as mid to southern Narrabeen-Collaroy, that frequently display complex bar morphology, to highly dissipative multiple bar sites in meso-tidal areas [42]. Generic relationships as a function of dimensionless fall velocity,  $\Omega$  [79], which relates wave characteristics and sediment grain size, were developed and presented. Specifically, for the 7 sites tested, there was a clear relationship between dimensionless fall velocity and the dominant modes of beach variability. Lower values of  $\Omega$ , indicative of lower energy intermediate and reflective beaches where sandbars are relatively close to shore [17], are linked to storm-dominated beaches that oscillated rapidly around a time-varying mean. In contrast, higher values of  $\Omega$ , representative of more high energy intermediate to dissipative beaches [17] are shown to oscillate at annual timescales around a time-invariant mean position. Blind testing of this generic model at a new site (Torrey Pines in California, USA) showed that the parameterized coefficients could successfully be used in the absence of sufficient training data.

#### 3.1.4. Shoreline Dynamics and the Role of Sandbars

A particular feature that is readily captured by video remote sensing but hard to obtain by in-situ instruments due to the obvious challenges of instrument deployment in the surfzone, is the time-varying location of the sandbar. Identified by wave breaking patterns averaged over 10-min (timex) images, sandbars are readily visible by preferential wave breaking patterns (i.e., white foam) in the images ([19]; for an example see Figure 5 this manuscript). As was noted earlier (Section 3.1.2) sandbars play a key role in the overall stability of the shoreline. During large wave events, sand is removed from the shoreline and deposited in offshore sandbars. During recovery, these sandbars slowly migrate back onshore, eventually welding to the shoreline, returning the sand to the subaerial beach. Using ten years of daily shoreline and sandbar position data derived from the permanent Narrabeen Argus station, Phillips et al. [74] detail and analyze rates of cross-shore sandbar migration and shoreline recovery following 82 individual storms. They found that at short timescales (i.e., in the days to weeks following a single storm event), shoreline recovery rates exhibit a high degree of temporal variability. Immediately post-storm, shoreline recovery rates are slow (between 0 and 0.2 m/day) as sand trapped in offshore sandbars slowly migrate back onshore. As sandbars near the shoreline, rates of shoreline recovery are 3 to 4 times higher (up to 2 m/day) as bars attach and weld to the shoreline, demonstrating the close link between observed rates of shoreline recovery and sediment availability. Interestingly, when shoreline recovery was examined over longer timescales (months), the average recovery rate between all 82 storms converged to ~0.2 m/day.

A number of studies from other sites around the world have similarly used video-derived data to examine the inter-dependency between shoreline and sandbar dynamics. For example, using over 9 years of observations from the Gold Coast, Australia, Price and Ruessink [43] and Splinter et al. [33] noted that when an offshore sandbar decayed during onshore migration following a large storm, it offered reduced protection to the shoreline and inner bar leading to enhanced erosion of the shoreline. At the embayed beach of Tairua, New Zealand, Blossier et al. [80] used 7 years of shoreline and sandbar data to examine the coupled dynamics of these morphological features. Using PCA analysis, the authors identified two dominant modes of variability at Tairua site: the first accounted for both migration and rotation of the observed shoreline and bar positions in opposing directions; and the second mode described the synchronous rotation of both these features.

### 3.2. Fixed Scanning Lidar

Laser scanners operate on the basic principle of time of flight to compute the distance between the target and sensor. Using this method of high frequency laser pulses, very high frequency and high spatial resolution data of various morphological and hydrodynamic features at beaches can be obtained. To date, data provided by the deployment of fixed lidar systems at the coast include a cross-shore 2D scan of the dune and dry beach profile, swash, and nearshore breaking waves [81–88]. The timescales of hydrodynamic and morphological processes that can be quantified and analyzed by these data extend from the shoreward propagation and runup at the beachface of an individual wave, through to the tide-by-tide and multi-year evolution of the subaerial beach and dunes. The accuracy of laser scanners is equivalent, if not better, than other common methods such as video cameras and in-situ ultrasonic sensors [89,90] that have been used for a similar purpose. For example, Brodie et al. [85] reported RMSE between lidar and pressure-based measurements between 0.03 m and 0.07 m for a range of surfzone hydrodynamic properties.

A fixed-scanning lidar was installed at Narrabeen-Collaroy adjacent to the permanent Argus camera station in July 2014 and has been scanning at 5 Hz continuously (night and day) since that time. A particular benefit of the fixed lidar system to compliment the additional visual information obtained by the co-located Argus video station at Narrabeen (Figure 7) is that beach and surfzone data collection is not restricted to only daylight hours. For example, Phillips et al. [84] reported on a 76-day continuous period following a major erosion event at Narrabeen. Sand volume changes across the sub-aerial beach obtained every semi-diurnal low tide (i.e., approximately twice per day) were most commonly between 1–2 m<sup>3</sup>/m/day, but these varied substantially and could be both accretive (positive) or erosive (negative) between consecutive tides. By comparison, the long-term average recovery rate was found to be 0.7 m<sup>3</sup>/m/day. Interestingly, the fixed lidar data captured a cyclic development and vertical growth of the berm. This repeated pattern, that occurred throughout the 76-day dataset, was shown to be linked to the spring-neap tidal cycle. Phillips et al. [84] identified four distinct modes of berm recovery within the Narrabeen dataset: Mode 1 beachface progradation (47% of the time) resulting in the lateral seaward migration of the berm face and often occurred during neap tides; Mode 2 beachface progradation with berm aggradation (22% of the time) associated with both a lateral seaward shift of the berm face as well as a vertical increase in the berm elevation and occurred during a rising tide cycle; Mode 3 beachface erosion with berm aggradation (15% of the time) caused by sand being moved from the lower beachface and deposited on the top of the berm during the spring tides; and lastly Mode 4 beachface erosion (15% of the time) that was observed to result in the offshore transport of sand from the beach face. This unique dataset provided from the fixed lidar was able to capture in unprecedented detail the temporal and spatial characteristics of beach and berm recovery over multiple spring-neap tide cycles.

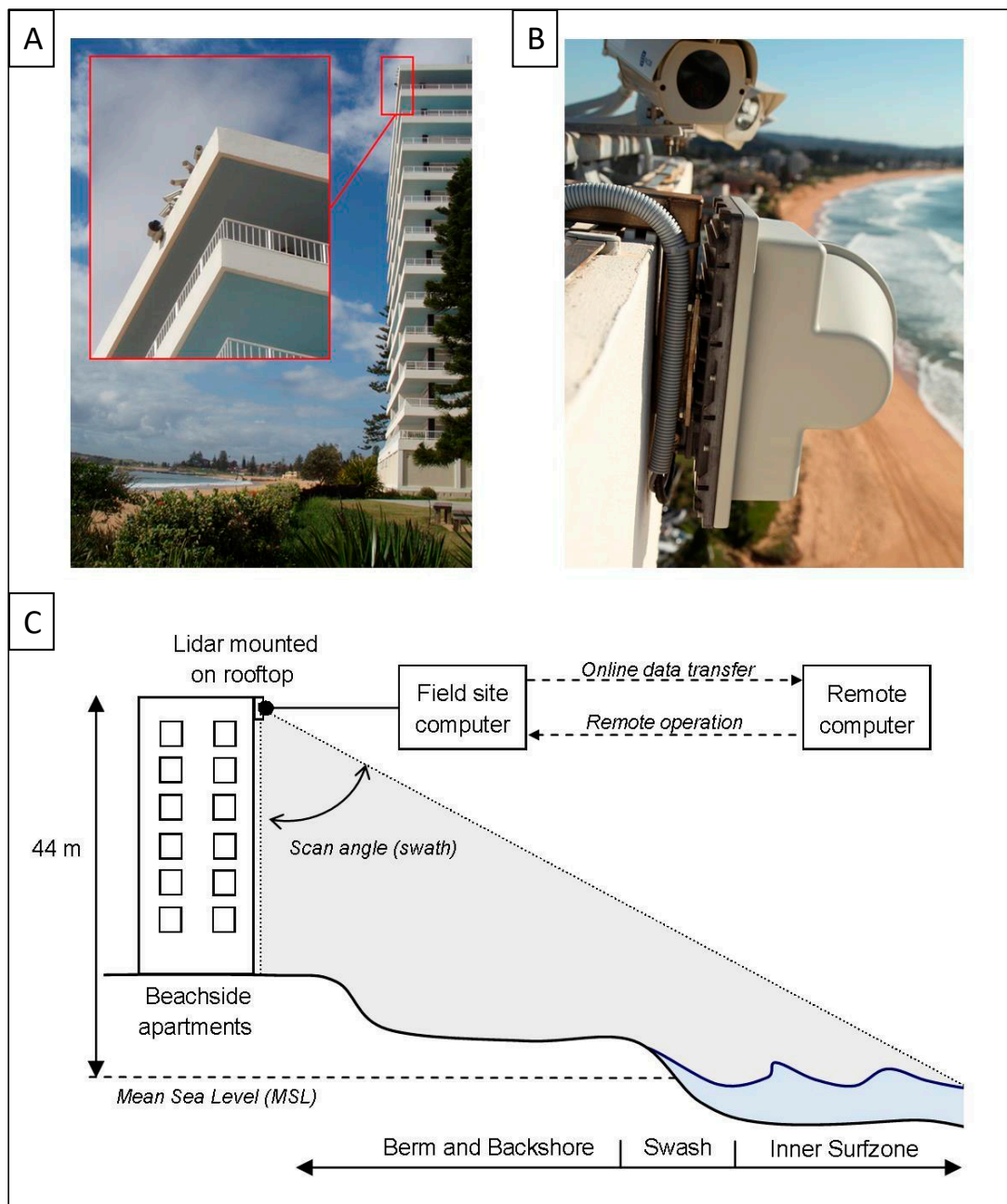


**Figure 7.** Fixed Lidar monitoring system photographs (A,B) showing Lidar instrument mounted on rooftop of beachside apartment building just below the Coastal Imaging station at Narrabeen-Collaroy Beach, SE Australia. (B) Schematic of lidar setup. Source: M. Phillips PhD Thesis (UNSW Sydney, 2018).

### 3.3. Surfcams

Recreational surf cameras (or ‘surfcams’) exist in many popular surf destinations around the world. These typically low elevation cameras are used for the qualitative assessment by surfers and other beach goers to estimate the size and quality of the surf, and often provide an income stream to their operators through online advertising. Using nine surfcams located along beaches in New South Wales including Narrabeen-Collaroy, Bracs et al. [91] examined if these existing camera networks could be repurposed to additionally provide routine image data (namely shorelines) equivalent to the more limited international network of research-focused camera systems, including Argus. At Narrabeen-Collaroy, comparison of the daily Argus-derived shorelines to those provided by the surfcam operator initially had a large standard deviation of error on the order of 6 m in the horizontal.

These findings agree with Splinter et al. [34] who reported large bias errors (~25 m) at 2 commercially operated sites at the Gold Coast using surfcams. However, Bracs et al. [91] reported that with proper calibration, including image geometry, improved shoreline detection, as well as rigorous quality controlling for shoreline visibility and rotating camera re-positioning, errors could be reduced to within 2 m. It was concluded that these low-cost systems can potentially deliver research quality data streams, provided there is close cooperation with their commercial operators. Their results also highlight that the application of remote sensing technologies to coastal science are only as good as the operators, and that robust data extraction methods are required to achieve the necessary quality of resulting data products.

Extending the potential application of existing surfcam networks to coastal science, Sanchez-Garcia et al. [92] recently presented a new tool, C-Pro (coastal projector) to project terrestrial images into georeferenced planes, explicitly using the horizon as a geometric constraint. These advanced geo-referencing techniques can better facilitate the use of existing low-elevation surfcams (or other recreational cameras, such as described in Section 3.4) with unknown image calibration to provide good quality, quantitative data. With networks of recreational cameras (including at the coast) continuing to grow rapidly, such tools will very likely play an increasing role in expanding the world-wide coastal monitoring, especially along more developed regions of the coastline.

#### 3.4. CoastSnap

Following the outcomes reported by Bracs et al. [91] whereby repurposed surfcams were shown to provide reasonable accuracy in shoreline detection provided suitable rectification and calibration was included, Harley et al. [93] have recently reported on the novel application of smartphones to obtain routine monitoring images of beaches. These crowd-sourced photos are supplied by the community back to researchers and managers via the digital media platforms Instagram, Twitter and Facebook. The first CoastSnap station was installed on the northern headland of the Narrabeen-Collaroy embayment in 2017 (Figure 1C), providing a new opportunity to observe the Narrabeen lagoon entrance and adjacent beach. The underlying concept of CoastSnap (<https://www.facebook.com/coastsnap>) is that a stainless-steel mounting bracket is installed at sites of interest to provide a fixed location and camera view angle, independent of the use of any particular smartphone. Community participants can then place their own phone in the bracket and take a snapshot image to upload to their preferred social media platform via the information provided at each CoastSnap location. Similar to an Argus camera station, permanent ground control points in the field of view are measured at the time of each CoastSnap installation, and used to georeference and rectify every image submitted by the public. However, where Argus cameras rely on fixed cameras with their intrinsic parameters previously determined, the various smartphone models for this crowd-sourced data collection means that camera intrinsics are instead approximated on-the-fly using the surveyed ground control points. Post-processing of the snapshot images includes shoreline detection (Figure 8A) based on a locally-adaptive threshold method using the difference between the red (sand) and blue (water) pixels. Since the initiation of CoastSnap, community participation has proven to be strong; for example, at the North Narrabeen site more than 220 images were provided by the public during the first six months of operation, equivalent to ~1 image/day. A comparison of data collected from the North Narrabeen CoastSnap station and in-situ surveys over this same 6-month period resulted in a cross-shore RMSE of 1.4 m for shorelines mapped close to the station in the camera nearfield, and RMSE = 3.9 m over nearly 1 km of beach. (Figure 8B). Interestingly, only marginal differences in shoreline accuracy were observed between low-resolution images uploaded using substantial image compression to social media (image resolution ~0.3 MP) and those sourced directly from the smartphone without any additional compression (image resolution > 2 MP). These promising results highlight the potential for this crowd-sourced data to be used more widely at beaches around the world for shoreline monitoring. At the time of writing, there are CoastSnap stations operating in Australia, Spain, Portugal and the UK, with further installations planned in several other countries including the USA and Brazil.

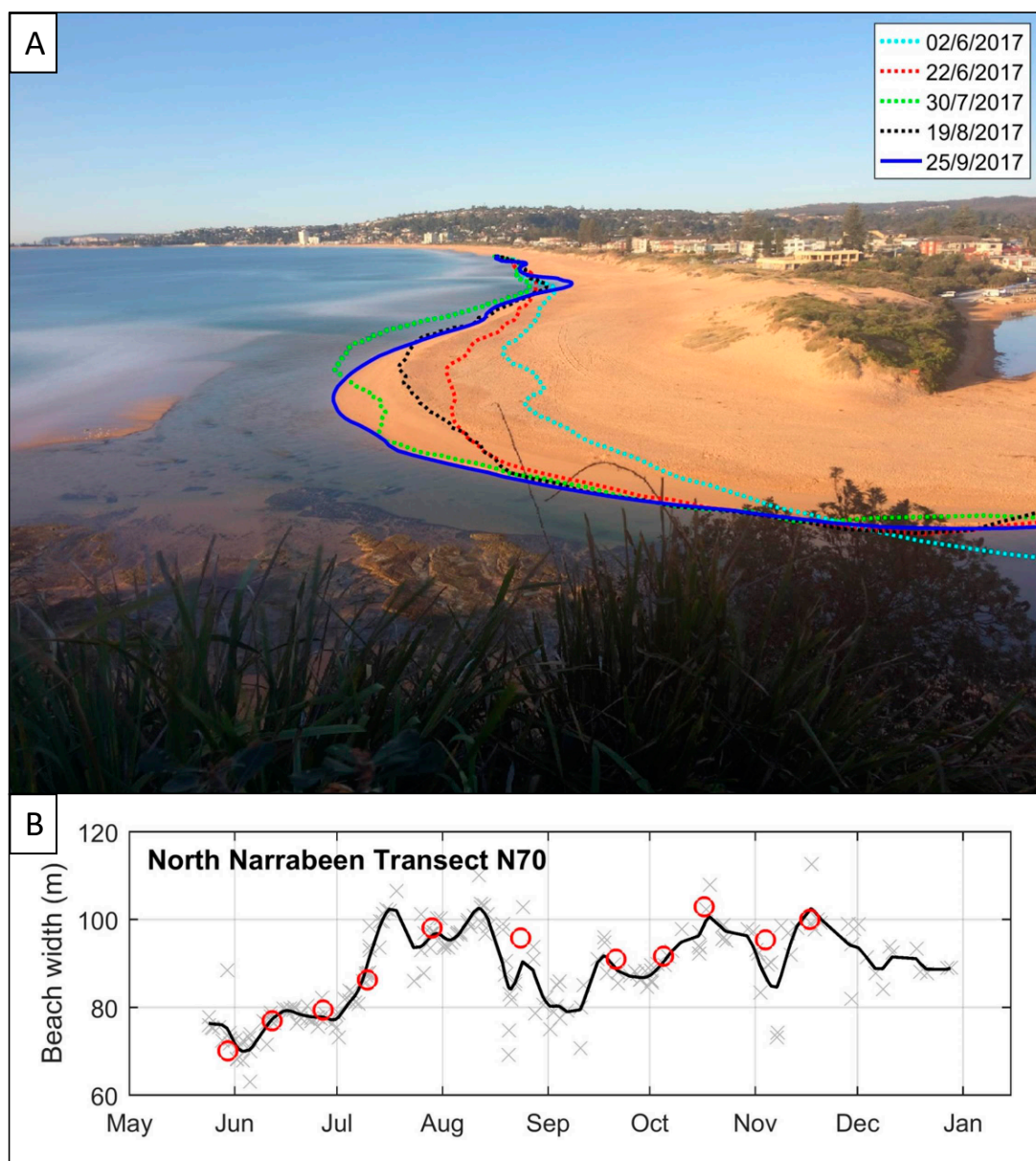


**Figure 8.** (A) Example figure showing shoreline change at North Narrabeen over a 3-month period 06/17–12/17. (B) Comparison of CoastSnap derived shorelines (grey and solid black line) to in-situ surveys (red dots).

### 3.5. Satellite-Derived Data

The increasing availability of satellite images (Figure 2) is opening up extensive new opportunities to perform long-term, routine coastline monitoring spanning large spatial scales [94,95]. Fortuitously, the 40+ year monitoring program at Narrabeen-Collaroy provides a robust and long-term dataset for evaluation and validation of satellite-derived products, including shoreline analyses. For example, Liu et al. [96] examined the use of super-resolution techniques applied to 29 years of Landsat images (resolution of 30 m pixel size) to derive nominally monthly, seasonal and annual trends in shoreline variability, and compared these directly to the Narrabeen dataset. After the Landsat images had been pan-sharpened, the super-resolution border segmentation method by Cipolletti et al. [97] was used to automatically extract shorelines at sub-pixel scale. Both the temporal and alongshore variability of individual shorelines at Narrabeen-Collaroy were found to be captured at sub-pixel accuracy with an RMSE <10 m, with the accuracy of annual-average shorelines further increasing to RMSE ~5 m.

The optimum use of satellite remote sensing for shoreline detection and analyses is still a developing area of research. For example, the use by Luijendijk et al. [94] of an alternative method in which yearly composite images and edge-detection/thresholding were used to delineate water from land, then a 1D Gaussian smoothing applied to the resulting shoreline signal, resulted in a reported RMSE of 14 m when they compared their results to the Narrabeen survey dataset.

Most recently, Vos et al. [98] applied new machine learning techniques to extend the methods of Liu et al. [96] to automatically detect shorelines from satellite images that are now freely available from the cloud (i.e., Landsat, ASTER, Sentinel-2) via the Google Earth Engine (<https://earthengine.google.com/>). Specifically, an image classification technique was applied to refine the sand/water interface. Using only those areas of identified water and sand and removing all other features, Ostu's method [99] was used to delineate the shoreline interface. Vos et al. [98] then compared their enhanced shoreline method to five long-term shoreline datasets from around the world including Narrabeen, where 502 individual satellite images between 1987–2018 are available. They report a cross-shore RMSE between satellite-derived and in situ (Emery method and RTK-GPS) shoreline measurements of 8.2 m (Figure 9B) at Narrabeen, comparable to the method of Liu et al. [96]. Interestingly, despite satellite resolution increasing over the last 30 years, no significant correlation to RMSE was found (Figure 9C). A timeseries comparison at Narrabeen profile 1 (northern most profile at Narrabeen) is illustrated in Figure 9A, showing an important new result that, by the application of machine learning methods, the satellite-derived data is capable of capturing storm-scale variability at this site, in addition to interannual shoreline behavior. Irrespective of the specific method applied, the suitability of 30 years of existing and freely-available satellite-derived data for coastline monitoring applications has now been established, especially where the primary focus is on longer-term, inter-annual signals of shoreline variability and change.

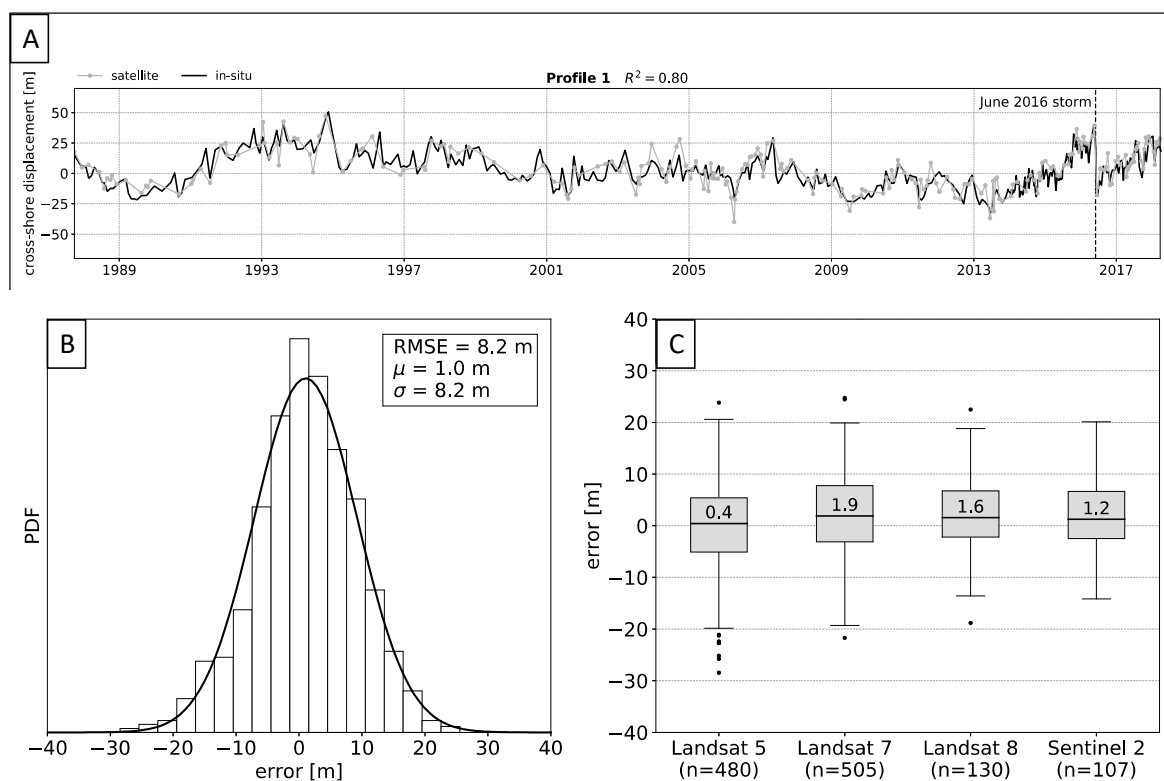


**Figure 9.** (A) timeseries comparison for profile 1; (B) Horizontal accuracy of the satellite-derived shorelines for Narrabeen (all 5 profiles); (C) boxplots of the error distribution as a function of satellite mission. Source: Vos et al. [98].

#### 4. Recent Developments: Enhanced Event-Based Monitoring (2011–Present)

While the routine and ongoing remote sensing techniques employed at Narrabeen continue to evolve as new technologies emerge and are refined by the wider scientific community, commencing in 2011 (Figure 2B), a significant new focus for the Narrabeen-Collaroy monitoring program was initiated, shifting from ‘routine’ measurements of the embayment using on-ground ATV and RTK-GPS, to an enhanced effort using remote sensing methods to quantify the rapid morphological impacts of individual storm events at the site, and the placing of these observations within their broader regional context. This required the development of new protocols facilitating the rapid deployment at short notice of remote-sensing instrumentation and personnel, such that pre- and post-storm measurements are now regularly achieved within 24 h of the onset and decline of targeted storm events. The particular survey focus is the dune and subaerial beach, with the use of aircraft-mounted airborne lidar and UAV providing both the regional-scale and more local survey capabilities required. A brief description of these recent additions to the remote-sensing tools and capabilities within the Narrabeen-Collaroy monitoring program are provided below.

##### 4.1. Airborne Lidar

Aircraft-mounted airborne lidar is a well established remote sensing tool that is now widely used to obtain high quality topographic data spanning large extents (100 s of kilometers) of coastline [100]. A rapid-response system to fly lidar for storm erosion monitoring was developed jointly by the University of New South Wales’ School of Aviation and Water Research Laboratory [101]. The airborne lidar system in use at Narrabeen incorporates a Piper Pa44 Seminole plane equipped with a Riegl Q240i lidar coupled with a NovAtel SPAN-CPT integrated GNSS and IMU. The plane is also equipped with a synchronized digital camera for visual images of the surveyed coast. Conveniently, the aircraft is permanently based at an airfield located 10 min flight time from Narrabeen, further facilitating very rapid deployment. Comparisons detailed in Middleton et al. [101] of in-situ ATV RTK-GPS surveys from Narrabeen showed the airborne lidar data had a mean vertical error of 0.02 m when outliers were removed. Using this new technology, the lidar system has repeatedly flown significant storm events between 2011 and present (Figure 2B); two of these events that illustrate the different capabilities of the system are described below.

In June 2011, lidar flights were undertaken daily at Narrabeen-Collaroy spanning a 6-day East Coast Low storm and captured for the first time, daily low-tide elevation data of the subaerial beach [102]. Unique to this data set, the rapid-response airborne lidar captured the alongshore variability in the immediate pre-storm beach morphology (including beach slope, dune height, and dune toe elevation) as well as the day-to-day changes throughout the storm. These unique daily lidar surveys revealed the considerable temporal, as well as alongshore, variability in the observed erosion as the storm progressed. The key drivers of alongshore variable dune erosion were linked to pre-storm morphology, specifically the dune toe elevation, rather than alongshore variability in wave conditions during this particular event.

In June 2016 an intense East Coast Low storm event impacted an extensive region of the east coast of Australia extending from Tasmania to southern Queensland, bringing heavy rains and the most extensive erosion observed in the 40 years of monitoring at Narrabeen-Collaroy [1,103]. Significantly expanding on the work by Bracs et al. [16] who focused on just two embayed beaches, pre- and post-storm airborne lidar surveys were flown along approximately 180 km of multiple sandy embayments spanning 400 km of the NSW coastline, including Narrabeen-Collaroy. From these pre- and post-storm surveys and a detailed analysis of the local inshore storm wave climate along this stretch of the coast, results revealed that the anomalous wave direction of the storm (which came from an easterly direction compared to the more usual south to south-easterly direction) was the main driver of the enhanced erosion seen throughout this 180 km stretch of embayed beaches. At the regional scale, alongshore gradients in erosion were also linked to alongshore gradients in storm wave energy flux and the relative alignment of the coastline [103].

Repeated regional-scale airborne lidar surveys since the June 2016 storm have also been used to begin to reveal the trends and drivers of regional-scale and longer-term beach recovery [104]. For example, the initial recovery of the subaerial beach along the 400 km of monitored coastline was observed to be rapid, with 35% of the eroded sand volume returning within the first 3 months. However, this rate did not continue, with only 51% recovery by 6 months and subsequent storms removing much of the initial recovery during the following 6-month period. In contrast, the upper beach (dune) had a very slow recovery at first (only 6% in the first 3 months) but continues to increase over time. Similar to the observed erosion that was significantly controlled by wave direction, this ongoing monitoring of the regional coastline is revealing significant spatial variability in the beach recovery response, with embayment orientation relative to the dominant wave direction emerging as a major control.

#### 4.2. Unmanned Aerial Vehicles

Unmanned Aerial Vehicles (UAVs—also commonly referred to as Unmanned Aerial Systems, or ‘drones’) are increasingly being used by coastal researchers and managers to monitor coastline variability and change. This remote sensing platform can provide dense, 3D point clouds of data that far exceed the spatial resolution that is captured by traditional in-situ methods described above. Since 2014 (Figure 2B), UAVs have been tested and verified against in-situ surveys at Narrabeen and are now used for event-based monitoring to compliment the regional-scale airborne lidar. Comparison between UAV-derived and ATV in-situ surveys showed a mean vertical offset  $<0.03$  m and a standard deviation  $<0.07$  m [105], which is within the range of accuracy of the RTK-GPS and comparable to other high-accuracy remote sensing methods such as airborne lidar [101]. The benefits of these systems to map a full embayment including the dune system, improves on the temporal and spatial constraints of the traditional in-situ surveys at a much-reduced cost and lead time to the airborne lidar.

Turner et al. [105] described the rapidly expanding use of fixed-wing UAV platforms for coastal surveying applications, using the Narrabeen-Collaroy monitoring program for illustration. In summary, ‘off-the-shelf’ survey quality UAVs incorporating onboard RTK-GPS for accurate positioning are now available, with parallel progress in computer vision—especially the development of sophisticated structure-from-motion methods [106] that permit the extraction of 3D topography from multiple overlapping images—providing survey data that is comparable in accuracy to both airborne lidar and on-ground RTK-GPS.

At the time of writing, the latest new remote-sensing development at Narrabeen is the use of UAV quadcopter platforms to facilitate the collection of video timestacks, that are then analyzed by the cBathy technique [27] to estimate time-evolving surfzone bathymetry [107]. Complimenting the exiting Argus station located in the southern part of the embayment, these newly available remote-sensed data obtained by UAV quadcopters now enable surfzone morphology to be monitored and quantified at any location alongshore, irrespective of a suitable beach-front building or other elevated location for the mounting of cameras. With UAV platforms and their remote sensing applications still in a rapid phase of development, the continuing expansion of their use at Narrabeen will no doubt occur.

### 5. Conclusions and Future Directions

Remote sensing methods are commonly and increasingly being used around the world to advance coastal science. At Narrabeen-Collaroy, today we pull in orders of magnitude more data in a single day than was obtained during the first decades when the monitoring program commenced more than 40 years ago. The deployment of a growing range of remote sensing tools and techniques has considerably advanced our understanding of beach processes at a range of temporal and spatial scales. For example, daily video remote sensing of the beach and nearshore sandbars over the past 1.5 decades reveal that antecedent morphology is a key driver in storm erosion response and beach recovery [31,32,72,74]. Daily video monitoring of the adjacent lagoon system at North Narrabeen showed that the morphodynamics of this intermittently open and closed coastal lake/lagoon entrance is controlled predominately by oceanic wave forcing [70]. In addition to video monitoring, continuous

fixed scanning lidar (2 Hz) over the past 4 years has provided new data that has been used to identify the dominant modes of subaerial berm recovery linked to spring-neap tidal cycles [84]. Since 2011, targeted event-based remote sensing methods such as airborne lidar and UAVs have provided unprecedented data that complements the long-term monitoring to understand the key drivers (antecedent morphology and wave exposure) of beach and dune erosion during storms over spatial scales of 100 s of meters to 100 s of kilometers [102,103] as well as regional scale beach recovery [104]. These scientific advances would not have been possible without remote sensing technology providing the necessary temporal and spatial scales required to observe and investigate these coastal phenomena.

As data becomes more accessible and digital storage cheaper, the quality and quantity of data that is collected will inevitably grow into the future. The technology used to collect data at Narrabeen has changed drastically since its humble beginnings of in-situ profile surveys using a rod and measuring tape. Today and into the future, new and emerging technologies including UAV, crowd-sourcing of data (e.g., CoastSnap), Google Earth Engine, and CubeSats will expand the frontiers on the data sources we collect and continue to improve understanding of coastal processes at event to decadal timescales into the future.

As new and expanding remote sensing technologies emerge, a key lesson from the existing monitoring program at Narrabeen is the importance of a regular re-evaluation of what data is most needed to progress the science. For example, understanding the key processes that drive swash and wave-by-wave sediment transport will still rely on methods, such as fixed scanning lidars and video from cameras, to capture data at high frequency and very localized spatial scales. On the other hand, satellite platforms, with lower overall spatial accuracy (but expected to continue to improve into the future), will offer unprecedented long-term datasets over 1000 s of kilometers of coastline, that will be critical to improving understanding of the impacts of present and future regional-scale climatic forcing on our coastlines. Crowd-sourced data may increasingly become the solution of choice to fill the gaps between these two spatial and temporal scales. Ultimately, we envisage a complementary suite of remote sensing products will be used together to enhance our understanding of the coastline into the future.

**Author Contributions:** K.D.S. wrote this review paper. M.D.H. and I.L.T. aided with the editing of this manuscript and providing additional details. All authors contributed to a variety of the research outcomes reviewed in this paper, as acknowledged by co-authorship in referenced journal publications.

**Funding:** Funding for the routine monitoring at Narrabeen is generously provided by Northern Beaches Council (formerly Warringah Council), UNSW Research Infrastructure Scheme, UNSW Faculty of Engineering Early Career Grant, the NSW Adaptation Research Hub—Coastal Processes Node (Office of Environment and Heritage), and the Australian Research Council (LP0455157, LP100200348, DP150101339, LP170100161). KD Splinter is also supported by the NSW Environmental Trust (RD2015/128). The CoastSnap pilot project at North Narrabeen was funded and supported by the NSW Office of Environment and Heritage.

**Acknowledgments:** The data collected as part of the Narrabeen long term monitoring program is a result of the tireless efforts of many past and present undergraduate and graduate students, as well as staff at both UNSW Sydney and U. Sydney. The authors wish to thank our friend and colleague Professor Andy Short for his initiative to start and maintain this program for as long as he did.

**Conflicts of Interest:** The authors declare no conflicts of interest.

## References

1. Turner, I.L.; Harley, M.D.; Short, A.D.; Simmons, J.A.; Bracs, M.A.; Phillips, M.S.; Splinter, K.D. A multi-decade dataset of monthly beach profile surveys and inshore wave forcing at Narrabeen, Australia. *Sci. Data* **2016**, *3*, 160024. [[CrossRef](#)] [[PubMed](#)]
2. Barnard, P.L.; Hubbard, D.M.; Dugan, J.E. Beach response dynamics of a littoral cell using a 17-year single-point time series of sand thickness. *Geomorphology* **2012**, *139–140*, 588–598. [[CrossRef](#)]
3. Pianca, C.; Holman, R.; Siegle, E. Shoreline variability from days to decades: Results of long-term video imaging. *J. Geophys. Res. C Ocean*. **2015**, *120*, 2159–2178. [[CrossRef](#)]

4. Kuriyama, Y.; Banno, M.; Suzuki, T. Linkages among interannual variations of shoreline, wave and climate at Hasaki, Japan. *Geophys. Res. Lett.* **2012**, *39*, 2–5. [[CrossRef](#)]
5. Emery, K.O. A simple method of measuring beach profiles. *Limnol. Oceanogr.* **1961**, *6*, 90–93. [[CrossRef](#)]
6. Short, A.D.; Trembanis, A.C.; Turner, I.L. Beach oscillations, rotation and the Southern Oscillation, Narrabeen Beach, Australia. In Proceedings of the 27th International Conference on Coastal Engineering (ICCE), Sydney, Australia, 16–21 July 2000; pp. 2439–2452.
7. Short, A.D.; Trembanis, A.C. Decadal scale patterns in beach oscillation and rotation Narrabeen Beach, Australia—Time series, PCA, and wavelet analysis. *J. Coast. Res.* **2004**, *20*, 523–532. [[CrossRef](#)]
8. Ranasinghe, R.; McLoughlin, R.; Short, A.; Symonds, G. The Southern Oscillation Index, wave climate, and beach rotation. *Mar. Geol.* **2004**, *204*, 273–287. [[CrossRef](#)]
9. Harley, M.D.; Turner, I.L.; Short, A.D.; Ranasinghe, R. Rotation and oscillation of an embayed beach. *Coast. Eng.* **2008**, *5*, 865–875.
10. Thomas, T.; Phillips, M.R.; Williams, A.T. Mesoscale evolution of a headland bay: Beach rotation processes. *Geomorphology* **2010**, *123*, 129–141. [[CrossRef](#)]
11. Barnard, P.L.; Short, A.D.; Harley, M.D.; Splinter, K.D.; Vitousek, S.; Turner, I.L.I.L.; Allan, J.; Banno, M.; Bryan, K.R.; Doria, A.; et al. Coastal vulnerability across the Pacific dominated by El Niño/Southern Oscillation. *Nat. Geosci.* **2015**, *8*, 1–8. [[CrossRef](#)]
12. Anderson, D.; Ruggiero, P.; Antolinez, J.A.A.; Mendez, F.J.; Allen, J. A climate index optimized for longshore sediment transport reveals interannual and multi-decadal littoral cell rotations. *J. Geophys. Res. Earth Surf.* **2018**, 1–24. [[CrossRef](#)]
13. Harley, M.D.; Turner, I.L.; Short, A.D.; Ranasinghe, R. A re-evaluation of coastal embayment rotation: The dominance of cross-shore versus alongshore sediment transport processes, Collaroy-Narrabeen Beach, SE Australia. *J. Geophys. Res.* **2011**, *116*, F04033. [[CrossRef](#)]
14. Harley, M.D.; Turner, I.L.; Short, A.D.; Ranasinghe, R. Assessment and integration of conventional, RTK-GPS and image-derived beach survey methods for daily to decadal coastal monitoring. *Coast. Eng.* **2011**, *58*, 194–205. [[CrossRef](#)]
15. Harley, M.D.; Turner, I.L.; Short, A.D. New insights into embayed beach rotation: The importance of wave exposure and cross-shore processes. *J. Geophys. Res. F Earth Surf.* **2015**, *120*, 1470–1484. [[CrossRef](#)]
16. Bracs, M.A.; Turner, I.L.; Splinter, K.D.; Short, A.D.; Mortlock, T.R. Synchronised patterns of erosion and deposition observed at two beaches. *Mar. Geol.* **2015**, *380*, 196–204. [[CrossRef](#)]
17. Wright, L.D.; Short, A.D. Morphodynamic variability of surf zones and beaches: A synthesis. *Mar. Geol.* **1984**, *56*, 93–118. [[CrossRef](#)]
18. Wright, L.D.; Short, A.D.; Green, M.O. Short-term changes in the morphodynamic states of beaches and surf zones: An empirical predictive model. *Mar. Geol.* **1985**, *62*, 339–364. [[CrossRef](#)]
19. Lippmann, T.C.; Holman, R.A. Quantification of sand bar morphology: A video technique based on wave dissipation. *J. Geophys. Res.* **1989**, *94*, 995–1011. [[CrossRef](#)]
20. Lippmann, T.C.; Holman, R.A. The spatial and temporal variability of sand bar morphology. *J. Geophys. Res.* **1990**, *95*, 11575. [[CrossRef](#)]
21. Masselink, G.; Short, A.D. The Effect of Tide Range on Beach Morphodynamics and Morphology: A Conceptual Beach Model. *J. Coast. Res.* **1993**, *9*, 785–800.
22. Aagaard, T.; Holm, J. Digitization of wave run-up using video records. *J. Coast. Res.* **1989**, *5*, 547–551.
23. Holman, R.A.; Stanley, J.; Özkan-Haller, H.T. Applying Video Sensor Networks to Nearshore Environmental Monitoring. *IEEE Pervasive Comput.* **2003**, *2*, 14–21. [[CrossRef](#)]
24. Holman, R.A.; Stanley, J. The history and technical capabilities of Argus. *Coast. Eng.* **2007**, *54*, 477–491. [[CrossRef](#)]
25. Holland, K.T.; Holman, R.A.; Lippmann, T.C.; Stanley, J.; Plant, N. Practical use of video imagery in nearshore oceanographic field studies. *IEEE J. Ocean Eng.* **1997**, *22*, 81–92. [[CrossRef](#)]
26. Turner, I.L.; Aarninkhof, S.G.J.; Holman, R.A. Coastal Imaging Applications and Research in Australia. *J. Coast. Res.* **2006**, *221*, 37–48. [[CrossRef](#)]
27. Holman, R.; Plant, N.; Holland, T. CBathy: A robust algorithm for estimating nearshore bathymetry. *J. Geophys. Res. Ocean* **2013**, *118*, 2595–2609. [[CrossRef](#)]
28. Alexander, P.S.; Holman, R.A. Quantification of nearshore morphology based on video imaging. *Mar. Geol.* **2004**, *208*, 101–111. [[CrossRef](#)]

29. Turner, I.L. Discriminating modes of shoreline response to offshore-detached structures. *J. Waterw. Port Coast. Ocean Eng.* **2006**, *132*, 180–191. [[CrossRef](#)]
30. Davidson, M.A.; Turner, I.L. A behavioral template beach profile model for predicting seasonal to interannual shoreline evolution. *J. Geophys. Res.* **2009**, *114*, F01020. [[CrossRef](#)]
31. Davidson, M.A.; Splinter, K.D.; Turner, I.L. A simple equilibrium model for predicting shoreline change. *Coast. Eng.* **2013**, *73*, 191–202. [[CrossRef](#)]
32. Splinter, K.D.; Turner, I.L.; Davidson, M.A.; Barnard, P.; Castelle, B.; Oltman-Shay, J. A generalized equilibrium model for predicting daily to interannual shoreline response. *J. Geophys. Res. Earth Surf.* **2014**, *119*, 1936–1958. [[CrossRef](#)]
33. Splinter, K.D.; Turner, I.L.; Reinhardt, M.; Ruessink, G. Rapid adjustment of shoreline behavior to changing seasonality of storms: Observations and modelling at an open-coast beach. *Earth Surf. Process. Landf.* **2016**. [[CrossRef](#)]
34. Splinter, K.D.; Strauss, D.R.; Tomlinson, R.B. Assessment of post-storm recovery of beaches using video imaging techniques: A case study at Gold Coast, Australia. *IEEE Trans. Geosci. Remote Sens.* **2011**, *49*, 4704–4716. [[CrossRef](#)]
35. Plant, N.G.; Holman, R.A.; Freilich, M.H. A simple model for interannual sand bar behavior. *J. Geophys. Res.* **1999**, *104*, 15755–15776. [[CrossRef](#)]
36. van Enckevort, I.M.J.; Ruessink, B.G. Video observations of nearshore bar behavior. Part 2: Alongshore non-uniform variability. *Cont. Shelf Res.* **2003**, *23*, 513–532. [[CrossRef](#)]
37. van Enckevort, I.M.J.; Ruessink, B.G.; Coco, G.; Suzuki, K.; Turner, I.L.; Plant, N.G.; Holman, R.A. Observations of nearshore crescentic sandbars. *J. Geophys. Res.* **2004**, *109*, 1–17. [[CrossRef](#)]
38. Ruessink, B.G.; Pape, L.; Turner, I.L. Daily to interannual cross-shore sandbar migration: Observations from a multiple sandbar system. *Cont. Shelf Res.* **2009**, *29*, 1663–1677. [[CrossRef](#)]
39. Castelle, B.; Ruessink, B.G.; Bonneton, P.; Marieu, V.; Bruneau, N.; Price, T.D. Coupling mechanisms in double sandbar systems. Part 1: Patterns and physical explanation. *Earth Surf. Process. Landf.* **2010**, *35*, 476–486. [[CrossRef](#)]
40. Pape, L.; Plant, N.G.; Ruessink, B.G. On cross-shore migration and equilibrium states of nearshore sandbars. *J. Geophys. Res. Earth Surf.* **2010**, *115*, 1–16. [[CrossRef](#)]
41. Splinter, K.D.; Holman, R.; Plant, N. A behavior-oriented dynamic model for sand bar migration and 2DH evolution. *J. Geophys. Res.* **2011**, *116*, C01020. [[CrossRef](#)]
42. Splinter, K.D.; Gonzalez, M.V.G.; Oltman-Shay, J.; Rutten, J.; Holman, R. Observations and modelling of shoreline and multiple sandbar behaviour on a high-energy meso-tidal beach. *Cont. Shelf Res.* **2018**, *159*, 33–45. [[CrossRef](#)]
43. Price, T.D.; Ruessink, B.G. State dynamics of a double sandbar system. *Cont. Shelf Res.* **2011**, *31*, 659–674. [[CrossRef](#)]
44. Price, T.D.; Ruessink, B.G. Observations and conceptual modelling of morphological coupling in a double sandbar system. *Earth Surf. Process. Landf.* **2013**, *38*, 477–489. [[CrossRef](#)]
45. Stockdon, H.F.; Holman, R.A. Estimation of wave phase speed and nearshore bathymetry from video imagery. *J. Geophys. Res.* **2000**, *105*, 22015. [[CrossRef](#)]
46. Aarninkhof, S.G.J. Nearshore Bathymetry Derived from Video Imagery. Ph.D. Thesis, Delft University, Delft, The Netherlands, 2003.
47. Holland, K.T.; Holman, R.A. Video estimation of foreshore topography using trinocular stereo. *J. Coast. Res.* **1997**, *13*, 81–87.
48. Plant, N.G.; Holman, R.A. Intertidal beach profile estimation using video images. *Mar. Geol.* **1997**, *140*, 1–24. [[CrossRef](#)]
49. Aarninkhof, S.G.J.; Roelvink, J.A. Argus-based monitoring of intertidal beach morphodynamics. *Proc. Coast. Sediments* **1999**, *99*, 2429–2444.
50. Aarninkhof, S.G.J.; Turner, I.L.; Dronkers, T.D.T.; Caljouw, M.; Nipius, L. A video technique for mapping intertidal beach bathymetry. *Coast. Eng.* **2003**, *49*, 275–289. [[CrossRef](#)]
51. Uunk, L.; Wijnberg, K.M.; Morelissen, R. Automated mapping of the intertidal beach bathymetry from video images. *Coast. Eng.* **2010**, *57*, 461–469. [[CrossRef](#)]

52. Didier, D.; Bernatchez, P.; Augereau, E.; Caulet, C.; Dumont, D.; Bismuth, E.; Cormier, L.; Floc'h, F.; Delacourt, C. LiDAR Validation of a Video-Derived Beachface Topography on a Tidal Flat. *Remote Sens.* **2017**, *9*, 1–22. [[CrossRef](#)]
53. Pianca, C.; Holman, R.; Siegle, E. Mobility of meso-scale morphology on a microtidal ebb delta measured using remote sensing. *Mar. Geol.* **2014**, *357*, 334–343. [[CrossRef](#)]
54. Harrison, S.R.; Bryan, K.R.; Mullarney, J.C. Observations of morphological change at an ebb-tidal delta. *Mar. Geol.* **2017**, *385*, 131–145. [[CrossRef](#)]
55. Holman, R.A.; Symonds, G.; Thornton, E.B.; Ranasinghe, R. Rip spacing and persistence on an embayed beach. *J. Geophys. Res. Ocean* **2006**, *111*. [[CrossRef](#)]
56. Turner, I.L.; Whyte, D.; Ruessink, B.G.; Ranasinghe, R. Observations of rip spacing, persistence and mobility at a long, straight coastline. *Mar. Geol.* **2007**, *236*, 209–221. [[CrossRef](#)]
57. Quartel, S. Temporal and spatial behaviour of rip channels in a multiple-barred coastal system. *Earth Surf. Process. Landf.* **2009**, *34*, 163–176. [[CrossRef](#)]
58. Holland, K.T.; Holman, R.A. Wavenumber-frequency structure of infragravity swash motions. *J. Geophys. Res.* **1999**, *104*, 13479–13488. [[CrossRef](#)]
59. Plant, N.; Holland, K.T.; Haller, M. Ocean Wavenumber Estimation from Wave-Resolving Time Series Imagery. *IEEE Trans. Geosci. Remote Sens.* **2008**, *46*, 2644–2658. [[CrossRef](#)]
60. Holman, R.A.; Chickadel, C.C. Optical remote sensing estimates of the incident wave angle field during NCEX. *Coast. Eng.* **2005**, *4*, 1072–1081.
61. Aarninkhof, S.G.J.; Ruessink, B.G. Video Observations and Model Predictions of Depth-Induced Wave Dissipation. *IEEE Trans. Geosci. Remote Sens.* **2004**, *42*, 2612–2622. [[CrossRef](#)]
62. Chickadel, C.C.; Holman, R.A.; Freilich, M.F. An optical technique for the measurement of longshore currents. *J. Geophys. Res.* **2003**, *108*, 3364. [[CrossRef](#)]
63. de Vries, S.; Hill, D.F.; de Schipper, M.A.; Stive, M.J.F. Remote sensing of surf zone waves using stereo imaging. *Coast. Eng.* **2011**, *58*, 239–250. [[CrossRef](#)]
64. Shand, T.D.; Bailey, D.G.; Shand, R.D. Automated Detection of Breaking Wave Height Using an Optical Technique. *J. Coast. Res.* **2012**, *28*, 671–682. [[CrossRef](#)]
65. Stockdon, H.F.; Holman, R.A. Accuracy of depth estimation techniques based on video observations of wave celerity. *Trans. Am. Geophys. Union* **1996**, *77*, 399.
66. Power, H.E.; Holman, R.A.; Baldock, T.E. Swash zone boundary conditions derived from optical remote sensing of swash zone flow patterns. *J. Geophys. Res. Ocean* **2011**, *116*. [[CrossRef](#)]
67. Senechal, N.; Coco, G.; Bryan, K.R.; Holman, R.A. Wave runup during extreme storm conditions. *J. Geophys. Res. Ocean* **2011**, *116*. [[CrossRef](#)]
68. Palmsten, M.L.; Splinter, K.D. Observations and simulations of wave runup during a laboratory dune erosion experiment. *Coast. Eng.* **2016**, *115*, 58–66. [[CrossRef](#)]
69. Palmsten, M.L.; Holman, R.A. Laboratory investigation of dune erosion using stereo video. *Coast. Eng.* **2012**, *60*, 123–135. [[CrossRef](#)]
70. Morris, B.D.; Coco, G.; Bryan, K.R.; Turner, I.L.; Street, K.; Vale, M. Video-derived mapping of estuarine evolution. *J. Coast. Res.* **2007**, *2007*, 410–414.
71. Harley, M.D.; Turner, I.L.; Short, A.D.; Ranasinghe, R. An empirical model of beach response to storms—SE Australia. In Proceedings of the 19th Australasian Coastal and Ocean Engineering Conference, Wellington, New Zealand, 16–18 September 2009; pp. 600–606.
72. Beuzen, T.; Splinter, K.D.; Marshall, L.A.; Turner, I.L.; Harley, M.D.; Palmsten, M.L. Bayesian Networks in coastal engineering: Distinguishing descriptive and predictive applications. *Coast. Eng.* **2018**, *135*, 16–30. [[CrossRef](#)]
73. Splinter, K.D.; Turner, I.L.; Davidson, M.A. How much data is enough? The importance of morphological sampling interval and duration for calibration of empirical shoreline models. *Coast. Eng.* **2013**, *77*, 14–27. [[CrossRef](#)]
74. Phillips, M.S.; Harley, M.D.; Turner, I.L.; Splinter, K.D.; Cox, R.J. Shoreline recovery on wave-dominated sandy coastlines: The role of sandbar morphodynamics and nearshore wave parameters. *Mar. Geol.* **2017**, *385*, 146–159. [[CrossRef](#)]

75. Gallop, S.L.; Harley, M.D.; Brander, R.W.; Simmons, J.A.; Splinter, K.D.; Turner, I.L. Assessing Cross-Shore and Alongshore Variation in Beach Morphology Due to Wave Climate: Storms to Decades. *Oceanography* **2017**, *30*. [[CrossRef](#)]
76. Kearney, E.T.; Harley, M.D.; Turner, I.L.; Wyeth, B.; Goodwin, I.D. An energy based model of storm induced shoreline erosion—Gold Coast, Australia. In *Coasts and Ports 2011: Diverse and Developing, Proceedings of the 20th Australasian Coastal and Ocean Engineering Conference and the 13th Australasian Port and Harbour Conference, Perth, Australia, 28–30 September 2011*; Engineers Australia: Sydney, Australia, 2011; pp. 191–196.
77. Splinter, K.D.; Carley, J.T.; Golshani, A.; Tomlinson, R. A relationship to describe the cumulative impact of storm clusters on beach erosion. *Coast. Eng.* **2014**, *83*, 49–55. [[CrossRef](#)]
78. Yates, M.L.; Guza, R.T.; O'Reilly, W.C. Equilibrium shoreline response: Observations and modeling. *J. Geophys. Res.* **2009**, *114*, C09014. [[CrossRef](#)]
79. Gourlay, M.R. *Beach and Dune Erosion Due to Storms*; Rep. No. M935/M936; Delft Hydraulics Laboratory: Delft, The Netherlands, 1968.
80. Blossier, B.; Bryan, K.R.; Daly, C.J.; Winter, C. Shore and bar cross-shore migration, rotation, and breathing processes at an embayed beach. *J. Geophys. Res. Earth Surf.* **2017**, *122*, 1745–1770. [[CrossRef](#)]
81. Brodie, K.L.; Slocum, R.K.; McNinch, J.E. New insights into the physical drivers of wave runup from a continuously operating terrestrial laser scanner. *Ocean* **2012**. [[CrossRef](#)]
82. Vousedoukas, M.I.; Kirupakaramoorthy, T.; Oumeraci, H.; de Torre, M.; Wübbold, F.; Wagner, B.; Schimmels, S. The role of combined laser scanning and video techniques in monitoring wave-by-wave swash zone processes. *Coast. Eng.* **2014**, *83*, 150–165. [[CrossRef](#)]
83. Martins, K.; Blenkinsopp, C.E.; Power, H.E.; Bruder, B.; Puleo, J.A.; Bergsma, E.W.J. High-resolution monitoring of wave transformation in the surf zone using a LiDAR scanner array. *Coast. Eng.* **2017**, *128*, 37–43. [[CrossRef](#)]
84. Phillips, M.S.; Blenkinsopp, C.E.; Splinter, K.D.; Harley, M.D.; Turner, I.L.; Cox, R.J. Beachface and berm morphodynamics of post-storm recovery: Observations using continuous scanning Lidar. *J. Geophys. Res. Earth Surf.* **2018**. in review.
85. Brodie, K.L.; Raubenheimer, B.; Elgar, S.; Slocum, R.K.; McNinch, J.E. Lidar and pressure measurements of inner-surfzone waves and setup. *J. Atmos. Ocean. Technol.* **2015**, *32*, 1945–1959. [[CrossRef](#)]
86. Almeida, L.P.; Masselink, G.; Russell, P.E.; Davidson, M.A. Observations of gravel beach dynamics during high energy wave conditions using a laser scanner. *Geomorphology* **2015**, *228*, 15–27. [[CrossRef](#)]
87. Martins, K.; Blenkinsopp, C.E.; Zang, J. Monitoring individual wave characteristics in the inner surf with a 2-dimensional laser scanner (LiDAR). *J. Sens.* **2016**. [[CrossRef](#)]
88. Hofland, B.; Diamantidou, E.; van Steeg, P.; Meys, P. Wave runup and wave overtopping measurements using a laser scanner. *Coast. Eng.* **2015**, *106*, 20–29. [[CrossRef](#)]
89. Blenkinsopp, C.E.; Mole, M.A.; Turner, I.L.; Peirson, W.L. Measurements of the time-varying free-surface profile across the swash zone obtained using an industrial LIDAR. *Coast. Eng.* **2010**, *57*, 1059–1065. [[CrossRef](#)]
90. Almeida, L.P.; Masselink, G.; Russell, P.; Davidson, M.; Poate, T.; McCall, R.; Blenkinsopp, C.; Turner, I. Observations of the swash zone on a gravel beach during a storm using a laser-scanner (Lidar). *J. Coast. Res.* **2013**, 636–641. [[CrossRef](#)]
91. Bracs, M.A.; Turner, I.L.; Splinter, K.D.; Short, A.D.; Lane, C.; Davidson, M.A.; Goodwin, I.D.; Pritchard, T.; Cameron, D. Evaluation of Opportunistic Shoreline Monitoring Capability Utilizing Existing “Surfcam” Infrastructure. *J. Coast. Res.* **2016**, *319*, 542–554. [[CrossRef](#)]
92. Sánchez-García, E.; Balaguer-Beser, A.; Pardo-Pascual, J.E. C-Pro: A coastal projector monitoring system using terrestrial photogrammetry with a geometric horizon constraint. *ISPRS J. Photogramm. Remote Sens.* **2017**, *128*, 255–273. [[CrossRef](#)]
93. Harley, M.D.; Kinsela, M.; Sanchez-Garcia, E.; Vos, K. Shoreline change mapping using crowd-sourced smartphone images. *Coast. Eng.* **2018**. in review.
94. Luijendijk, A.; Hagenaars, G.; Ranasinghe, R.; Baart, F.; Donchyts, G.; Aarninkhof, S. The State of the World’s Beaches. *Sci. Rep.* **2018**, *8*, 1–11. [[CrossRef](#)] [[PubMed](#)]
95. Mentaschi, L.; Vousedoukas, M.I.; Pekel, J.-F.; Voukouvalas, E.; Feyen, L. Global long-term observations of coastal erosion and accretion. *Sci. Rep.* **2018**, *8*, 12876. [[CrossRef](#)] [[PubMed](#)]

96. Liu, Q.; Trinder, J.; Turner, I.L. Automatic super-resolution shoreline change monitoring using Landsat archival data: A case study at Narrabeen–Collaroy Beach, Australia. *J. Appl. Remote Sens.* **2017**, *11*, 016036. [[CrossRef](#)]
97. Cipolletti, M.P.; Delrieux, C.A.; Perillo, G.M.E.; Piccolo, M.C. Superresolution border segmentation and measurement in remote sensing images. *Comput. Geosci.* **2012**, *40*, 87–96. [[CrossRef](#)]
98. Vos, K.; Splinter, K.D.; Harley, M.D.; Simmons, J.A.; Turner, I.L. Sub-annual to multi-decadal shoreline variability from publicly available satellite imagery. *Coast. Eng.* **2018**. in review.
99. Otsu, N. OTSU paper. *IEEE Trans. Syst. Man Cybern.* **1979**, *20*, 62–66. [[CrossRef](#)]
100. Sallenger, A.J.; Krabill, W.B.; Swift, R.N.; Brock, J.; List, J.H.; Hansen, M.; Holman, R.A.; Manizade, S.; Sontag, J.; Meredith, A.; et al. Evaluation of airborne topographic lidar for quantifying beach changes. *J. Coast. Res.* **2003**, *19*, 125–133.
101. Middleton, J.H.; Cooke, C.G.; Kearney, E.T.; Mumford, P.J.; Mole, M.A.; Nippard, G.J.; Rizos, C.; Splinter, K.D.; Turner, I.L. Resolution and accuracy of an airborne scanning laser system for beach surveys. *J. Atmos. Ocean. Technol.* **2013**, *30*, 2452–2464. [[CrossRef](#)]
102. Splinter, K.D.; Kearney, E.T.; Turner, I.L. Drivers of alongshore variable dune erosion during a storm event: Observations and modelling. *Coast. Eng.* **2018**, *131*, 31–41. [[CrossRef](#)]
103. Harley, M.D.; Turner, I.L.; Kinsela, M.A.; Middleton, J.H.; Mumford, P.J.; Splinter, K.D.; Phillips, M.S.; Simmons, J.A.; Hanslow, D.J.; Short, A.D. Extreme coastal erosion enhanced by anomalous extratropical storm wave direction. *Sci. Rep.* **2017**, *7*, 6033. [[CrossRef](#)] [[PubMed](#)]
104. Harley, M.D.; Turner, I.L.; Middleton, J.H.; Kinsela, M.A.; Hanslow, D.; Splinter, K.D.; Mumford, P. Observations of beach recovery in SE Australia following the June 2016 east coast low. In Proceedings of the Australasian Coasts & Ports 2017: Working with Nature, Cairns, Australia, 21–23 June 2017; p. 559.
105. Turner, I.L.; Harley, M.D.; Drummond, C.D. UAVs for coastal surveying. *Coast. Eng.* **2016**, *114*, 19–24. [[CrossRef](#)]
106. Westoby, M.J.; Brasington, J.; Glasser, N.F.; Hambrey, M.J.; Reynolds, J.M. “Structure-from-Motion” photogrammetry: A low-cost, effective tool for geoscience applications. *Geomorphology* **2012**, *179*, 300–314. [[CrossRef](#)]
107. Holman, R.A.; Brodie, K.L.; Spore, N.J. Surf Zone Characterization Using a Small Quadcopter: Technical Issues and Procedures. *IEEE Trans. Geosci. Remote Sens.* **2017**, *55*, 2017–2027. [[CrossRef](#)]



© 2018 by the authors. Licensee MDPI, Basel, Switzerland. This article is an open access article distributed under the terms and conditions of the Creative Commons Attribution (CC BY) license (<http://creativecommons.org/licenses/by/4.0/>).